TECHNISCHE UNIVERSITÄT WIEN

DIPLOMARBEIT

Method for the evaluation of the performance of a multi-channel nerve cuff electrode coupled with a transcutaneous transfer array

zur Erlangung des akademischen Grades

Diplom-Ingenieur

Im Rahmen des Studiums

Physikalische Energie- und Messtechnik

eingereicht von

Emil Ogrodnik

Matrikelnummer 01428430

ausgeführt am Institut für Angewandte Physik

der Fakultät für Physik der Technischen Universität Wien

in Zusammenarbeit mit dem Zentrum für Medizinische Physik und Biomedizinische Technik der Medizinischen Universität Wien

Betreuer:

Ao.Univ.Prof. Dipl.-Ing. Dr.techn. Martin Gröschl, Institut für Angewandte Physik, Technische Universität Wien

und

Dipl.-Ing. Dr. Martin Schmoll, BSc, Zentrum für medizinische Physik und Biomedizinische Technik, Medizinische Universität Wien

Wien, 12.05.2022 _____ _____

(Unterschrift Verfasser) (Unterschrift Betreuer)

1 Acknowledgements

I would like to thank all people and parties that made this work possible. I would like to thank my supervisor Prof. Gröschl from the Technical University in Vienna for enabling and overseeing this work. I would like to thank Dr. Martin Schmoll from the Medical University in Vienna for his exceptionally patient and thorough guidance, advice and encouragement throughout the entire project.

I also want to thank Prof. Aszmann and his team from the Department of Plastic, Reconstructive and Aesthetic surgery and the entire team from the Imtek, University of Freiburg for letting me join in and be part of their project as well as Ottobock Healthcare. I would especially like to thank Gregor Längle, MD for performing all surgeries and providing medical oversight during this project.

Further I want to thank Mrs. Carina Brunnhofer for her beautiful artwork and her permanent support in all aspects of writing this work.

I would like to thank my parents Czeslaw and Barbara for laying the foundation of my academic career and their never ending patience and unconditional support. My brother Michael for providing just the right amount of competition and support.

I would like to thank Mag. Werner Schalko for building on that foundation. Who, leading by example, showed me the fruits of hard work and the joy of success as well as the necessity of a team of good people around you.

Szczególne dzieki chciałbym też złożyć pani Alfredzie Wolskiej i calej rodzinie za opieke, ćierpliwość i szczere zainteresowanie mną i mojimi studiami.

Table of Contents

2 Abstract

Introduction

A multi-channel nerve cuff electrode can be used to elicit selective contractions of different muscles depending on the position of the stimulating electrode. The stimulation current evokes action potential in the nerve fibres which is passed on to the attached muscles and results in contraction. Depending on the configuration of the fascicles, the different channels of the nerve cuff electrode will preferably address different muscles, allowing for selective control of movement.

Materials and methods

A method for the evaluation of a system for the selective stimulation of the gastrocnemius and the tibialis anterior muscles was developed. The system consisted of a multi-channel nerve-cuff electrode wrapped around the sciatic nerve and a coupling array, which allowed for the resistive transfer of current through the skin. These components were connected and could be assessed separately through a headstage port. The system was implanted in 10 female Sprague Dawley rats and tested under *in vivo* conditions. Measurements were performed to determine the current distribution on the channels of the transfer array as well as the selectivity of the different channels in the nerve cuff electrode with respect to stimulating only the gastrocnemius muscle or only the tibialis anterior muscle. Additionally measurements of the entire system were performed. The experiments were performed over a duration of 12 weeks after surgery. Two models were developed, to estimate the necessary array performance using the results from the measurements of the cuff electrode.

Results

Most subjects did not survive for the duration of the experiment. The mean lifespan amounted to 33 days (SD = 25 days) after surgery, not taking into account the animals that died on the day of surgery. Only one animal survived for the intended duration. Due to the rats movement mechanical failure was observed in 6 out of 8 animals, reducing the amount of performed experiments further As the mechanical failure usually only prevented measurements of a single component, the remaining system was still examiined. The mean time for the first mechanical failure to be detected was 24 days (SD= 11 days). Crosstalk coefficients between 73% and 115% were observed, where values above 100% mean, that the secondary channel received more current than the primary channel (lower numbers signify a better performance). The measurements of the nerve cuff electrode were used to estimate the necessary crosstalk coefficients to achieve selective behaviour in the full system. The more optimistic model, which assumed two separate stimulation sites to be fully independent, estimated the necessary crosstalk coefficient to be below 52% for any selectivity to be possible and below 37% for the coupling array to no longer be the limiting component for the performance. The second model which assumed a linear interaction between two stimulation sites estimated crosstalks coefficients below 23% to be necessary for the function of the system. Stimulation with the full system was possible, however the measurements of the full system did not show any selective behaviour, which matches the expectations from the results of the separate components.

Discussion

The sample size was drastically reduced due to the high amount of mechanical failures and the short life expectancy of the test subjects. The implementation in an *in vivo* subject proved to be technically problematic due to the size and stability of the implant. The performance of the electrode array was worse than under previously published *ex vivo* conditions and was insufficient for the system as a whole to perform selectively. However we were able to show selective behaviour of the nerve cuff electrode and develop a method to estimate the necessary crosstalk coefficient of the input signal. The results of the cuff measurements are in line with the work of previous authors, who performed similar experiments using steering currents. This is a technique that should be strongly considered in the further development. Further *in vivo* experiments should be postponed until the performance of the electrode array matches the thresholds defined by the models using the data from the cuff measurements. In addition to improving the performance of the system, the biocompatibility of the implant needs to be improved, so that the test subjects can survive for the intended duration. This would require a redesign, ideally including a reduction in size as well as eliminating elements protruding the skin. The performance of the nerve cuff electrode can be studied more thoroughly in a smaller implant to provide more precise values for the required crosstalk coefficient benchmarks without the need of implanting the entire system.

3 Zusammenfassung

Durch das Platzieren einer Manschettenelektrode (Cuff-Elektrode) mit mehreren Kanälen um einen Nerv wird eine selektive Kontraktion von Muskeln ermöglicht, die von der Position des stimulierenden Kanals abhängig ist. Der stimulierende Strom bewirkt im Nerv die Bildung eines Aktionspotentials, welches den Nerv entlang geleitet wird und den zugehörigen Muskel stimuliert und Kontraktionen auslöst. Je nach Aufteilung der Faszikelbündel werden unterschiedliche Muskeln von verschiedenen Kanälen bevorzugt, was eine selektive Ansteuerung möglich macht.

Es wurde eine Methode zur Bewertung eines Systems zur selektiven Stimulation der *Gastrocnemius* und des *Tibialis Anterior* Muskeln entwickelt. Dieses System bestand aus einer Cuff-Elektrode mit mehreren Kanälen, die um den Ischiasnerv positioniert war, sowie aus einem Elektrodenarray zum Einkoppeln des Stimulationsstroms durch die Haut. Diese Komponenten waren durch einen Stecker am Kopf des Tieres verbunden, und konnten durch diesen auch separat angesteuert werden. Das System wurde in zehn weiblichen Sprague Dawley Ratten implantiert und unter *in vivo* Bedingungen untersucht. Es wurden Messungen durchgeführt, um die Stromverteilung im Elektrodenarray zu ermitteln, sowie Messungen zur Bestimmung der erreichbaren Selektivität an den verschiedenen Kanälen der Cuff-Elektrode im Bezug auf die Anregung des *Gastrocnemius* und des *Tibialis Anterior*. Zusätzlich wurden Messungen zur Bestimmung der Selektivität des Gesamtsystems durchgeführt. Die Versuche wurden über einen Zeitraum von 12 Wochen nach der Implantation durchgeführt. Es wurden zwei Modelle entwickelt, um aus den Messungen der Cuff-Elektrode jene Stromaufteilung für das Elektrodenarray zu schätzen, bei der eine selektive Ansteuerung beider Muskeln noch möglich ist.

Die meisten Versuchstiere überlebten nicht die gesamte Dauer der Experimente. Die durchschnittliche Lebensdauer betrug 33 Tage (std. Abw.= 25 Tage) nach der Operation, wobei Tiere, die am Tag des Eingriffs verstorben sind, hierbei nicht berücksichtigt wurden. Nur ein Tier überlebte für die gesamte vorgesehene Dauer. Aufgrund der Bewegung der Ratte kam es häufig zu mechanischen Versagen diverser Komponenten im System. Dies verhinderte manche Teilmessungen während der Experimente, allerdings konnten Messungen der intakten Komponenten weiterhin durchgeführt werden. Die durchschnittliche Zeit zum ersten Ausfall einer Komponente betrug 24 Tage (std. Abw.= 24 Tage). Es wurden „*Crosstalk Koeffizienten*“ des Elektrodenarrays zwischen 73% und 115% gemessen, wobei Werte über 100% bedeuten, dass mehr Strom am sekundären Kanal als am Primären Empfangen wurden (kleine Werte entsprechen einer besseren Leistung des Arrays). Die Ergebnisse der Messungen der Cuff-Elektrode wurden in zwei Modellen zur Schätzung des Crosstalk-Koeffizienten verwendet, bei dem das Gesamtsystem selektives Verhalten aufweist. Das optimistischere Model nimmt an, dass die gleichzeitige Stimulation an mehreren Kanälen vollständig unabhängig ist und liefert einen Grenzwert von 52% für den Crosstalk-Koeffizienten, bei dem die selektive Ansteuerung beider Muskeln möglich ist. Ab einem Grenzwert von 37% ist das Elektrodenarray nicht mehr die limitierende Komponente und ein weiteres Herabsenken des Crosstalk Koeffizienten verbessert die Selektivität des Gesamtsystems nicht mehr. Im zweiten Model wird ein linearer Zusammenhang zwischen zwei gleichzeitig stimulierenden Kanälen angenommen und ein Grenzwert von 23% errechnet, ab dem das Gesamtsystem selektives Verhalten aufweist. Eine Stimulation mit dem Gesamtsystem war möglich,

allerdings konnte kein selektives Verhalten beobachtet werden, was mit den Erwartungen aus den Ergebnissen der Einzelmessungen im Einklang steht.

Die Stichprobengröße wurde durch die kurze Lebensdauer und das zahlreiche mechanische Versagen drastisch reduziert. Die Implementierung in eine *in vivo* Umgebung erwies sich technisch als große Herausforderung. Die Leistung des Elektrodenarrays war schlechter als unter zuvor veröffentlichten *ex vivo* Bedingungen und erwies sich als unzureichend um eine selektive Ansteuerung durch das Gesamtsystem zu erlauben. Allerdings waren wir in der Lage, selektives Verhalten der Cuff-Elektrode zu beobachten und eine Methode zu entwickeln, um den notwendigen Crosstalk-Koeffizienten des Eingangssignals zu bestimmen. Die Ergebnisse der Messungen der Cuff Elektrode sind im Einklang mit den Resultaten anderer Autoren, die ähnliche Experimente durchgeführt haben und in der Lage waren, mithilfe von zusätzlichen Lenkströmen die Selektivität der Elektrode noch weiter zu verbessern. Diese Technik sollte für die weitere Entwicklung des Systems in Betracht gezogen werden. Weitere *in vivo* Experimente sollten erst durchgeführt werden, wenn das Elektrodenarray die ermittelten Grenzwerte erfüllt. Außerdem muss die Biokompatibilität des Implantats verbessert werden, sodass die Versuchstiere die gesamte Dauer des Experiments überleben. Dafür muss das Implantat neu gestaltet werden, wobei idealerweise die Größe reduziert und auf Elemente die die Haut durchstoßen verzichtet wird. Das Verhalten der Cuff-Elektrode kann mit einem kleineren Implantat genauer untersucht werden und somit genauere Grenzwerte liefern, ohne das gesamte System implantieren zu müssen.

4 List of abbreviations

AP	Action potential
ATP	Adenosine triphosphate
CMAP	Common muscle action potential
CP	Common peroneal nerve
DAQ	Data acquisition
EMG	Electromyography
FES	Functional electrical stimulation
G	Gastrocnemius muscle
LG	Lateral gastrocnemius
MG	Medial gastrocnemius
SD	Standard deviation
TA	Tibialis anterior muscle
TET	Transcutaneous energy transfer
Tib	Tibial nerve

5 List of symbols

Equation 1 and 3

E	Nernst voltage	[V]	
c	Concentration	[mol/l]	
R = 8.314	Gas constant	[J/(mol K)]	
F = 96485	Faraday constant	[As/mol]	
z	Number of electrons transferred	[1]	
T	Temperature	[K]	
V_m	Voltage over membrane	[V]	
$k_B = 1.38 \cdot 10^{-23}$	Boltzmann constant	[J/K]	
$q = 1.6 \cdot 10^{-19}$	Elementary charge	[C]	
P_i	Permeability of i	[1]	$i \in \{ K^+, Na^+, Cl^- \}$
[i]	Concentration of i	[mol/L]	$i \in \{ K^+, Na^+, Cl^- \}$

Equation 7 - 12

c_{high}	Higher crosstalk limit	[1]	
c_{low}	Lower crosstalk limiting	[1]	
$I_{thr,id1,id2}$	Threshold current	[mA]	

id1 ∈ { G: gastrocnemius; TA: tibialis anterior }

id2 ∈ { 1: "gastrocnemius is primary muscle"; 2: "tibialis anterior is the primary muscle" }

I_1	Current on channel 1	[mA]	
I_2	Current on channel 2	[mA]	
c_{M2}	Crosstalk coefficient for Model 2	[1]	

Figure 6

i_m	Current over the membrane	[mA]	
i_i	Ionic currents	[mA]	
i_c	Capacitive currents	[mA]	

6 Introduction

6.1 Neurons

Neurons are the cells in our nervous system which receive, conduct and transmit nerve impulses[1]. Nerve cells (neurons) consist of a cell body (soma) with dendrites branching out as well as one long axon. Most of the neuron cell bodies are located in the brain, the spinal cord and ganglia. This is referred to as the central nervous system. The dendrites are connected to other neurons and "listen" for stimuli in the form of synaptic impulses from connected neurons. Figure 1 shows a motor neuron which is responsible for the bodies movement. These cells pass on information from the central nervous system to the bodies muscles and evoke controlled contractions of the muscles.

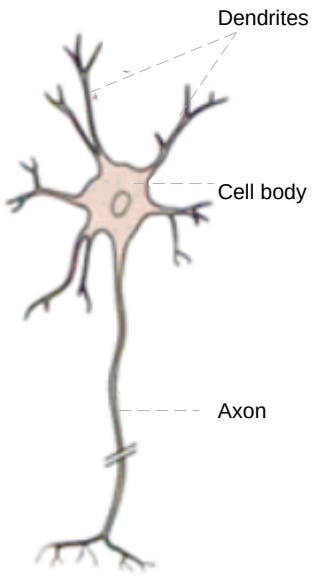

Figure 1: Anatomy of a motor neuron. Figure taken from Kandel et al.[4]

If the total synaptic impulse received by the dendrites and the cell body is above a certain threshold, the neuron will react, by sending it's own stimulus, i.e. action potential (AP), along the axon. The stimulus is generated in the axon hillock, which is the place the axon joins the soma[2]. While there can be a large number of dendrites, each neuron can have only one axon. The length of an axon can vary, depending on the target. The longest axons reach from the lower spine to the toes and can have lengths of well over a metre[2]. An important parameter for axons is their conduction speed of signals. Axons with large diameters conduct signals faster than those with a small diameter, as the conductivity is inversely related to the cross section area[2]. The speed can range from a few centimeters per second to 100 m/s for the largest axons which are found in squids[2]. Many axons are covered in a myelin sheath to further improve the conduction speed without increasing the necessary space. The myelin sheath insulates the axon partly from the outside, allowing for the depolarisation current to travel further bringing more distant regions of the axon above the stimulation threshold sooner[2].

The axon branches out at its end, allowing it to contact more than one target. The point of contact is called a synapse, and it allows for communication through the transfer of electric signals or a neurotransmitter. There are many highly specialised types of neurons, which can be roughly classified into:

Afferent neurons: These transport sensory information from the periphery to the central nervous system.

Efferent neurons: These send commands from the central nervous system to the muscles and organs.

Interneurons: These neurons pass information between neurons.

A neuron integrates excitatory and inhibitory synaptic potential received via the dendrites, and decides, whether the sum of these signals is above a certain threshold. If the threshold is crossed, an action potential is passed down the axon. The neurons are only capable of an "all-or-nothing" response. This means that there is no reaction below the threshold and a full reaction, as soon as it is passed.

6.2 Membrane voltage

Communication throughout the body can be achieved through bioelectrical signals, which are referred to as action potentials. Nerve cells produce and propagate these action potentials by an imbalance of charged ions (mainly Sodium Na^+, Potassium K^+ and Chlorine Cl^-) on the inside and the outside of the cell membrane. The potential across a permeable membrane is described by the Nernst equation[3]:

$$E = \frac{RT}{zF} \ln \frac{c_{outside}}{c_{inside}}$$

Equation 1: Nernst equation[3]

In equation 1 R = 8.314 J/molK refers to the gas constant, F = 96485 As/mol refers to the Faraday constant and z refers to the number of electrons exchanged per reaction. T is the temperature in K and c refers to the concentration in mol/l. Using the concentrations of all ion species which can be determined by the Nernst potential of each species (table 1).

Ion concentrations in and around the cell			
Ion	**Concentration in cytoplasm**	**Concentration in extracellular fluid**	**Nernst potential**
	[mmol/l]	**[mmol/l]**	**mV**
K+	400	20	-75
Na+	50	440	+55
Cl-	52	560	-60

Table 1: Concentration and equilibrium potential of ions in and around the cell[4]

To reach a constant resting potential a membrane needs to be in a state of steady flux. This means that the outward flux of K^+ ions needs to balance out the inward flux of Na^+ ions and the outward flux of Cl^- ions[4]. This resting point lies around -60 mV, which is very close to the Nernst potential of potassium but far away from the Nernst potential of sodium in most nerve cells[4]. The position of

this balance point can be explained by the relationship of the ion flux with the driving force and the conductance over the membrane:

$$\text{ion flux} = (\text{chemical driving force} + \text{electrical driving force}) \times \text{conductance across membrane}$$

Equation 2: ion flux[4]

An ion species with a higher conductance can achieve the same flux with a smaller driving force (i.e. potential difference towards equilibrium potential). Therefore the permeability of K^+ ions can be expected to be higher than the permeability of Na^+ ions. This observation matches the outcome of experiments conducted with radioactive tracers[4].

The membrane voltage can be described by the Goldmann equation (equation 3)[5]. The form of the Goldmann equation is similar to that of the Nernst equation. However it additionally takes the differing permeabilities of the ions through the cell membrane into account[5]. The Goldmann equation describes states of constant membrane potential, i.e. steady ion flux, which is the case during the resting state, but also during the peak of an action potential, where there is an instant in time, during which V_m doesn't change and the Goldmann equation is applicable[4].

$$V_m = \frac{k_b T}{q} \ln\left(\frac{P_K[K^+]_o + P_{Na}[Na^+]_o + P_{Cl}[Cl^-]_i}{P_K[K^+]_i + P_{Na}[Na^+]_i + P_{Cl}[Cl^-]_o}\right)$$

Equation 3: Goldmann equation[5]

P_i refers to the permeability of the ion species *i* through the cell membrane, $k_B = 1.38 * 10^{-23}$ *J/K* is the Boltzmann constant, q = 1.6 * 10^{-19} C is the charge of an electron, the index *o* refers to *outside of the cell* and the index *i* refers to *inside the cell*. The temperature in all further calculations is T = 298 K.

The cell membrane consist of a lipidic bilayer which can be seen in figure 2. A lipid is a long molecule containing a hydrophobic head and a hydrophilic ending. By aligning the hydrophobic endings to the inside of the bilayer, the lipids form a barrier, which polar components such as ions can not pass. Ions can only pass the cell membrane via specific ion channels. These channels have different ion permeability for the different ion types, strongly favouring potassium meaning that potassium ions can pass the membrane easier than sodium ions.

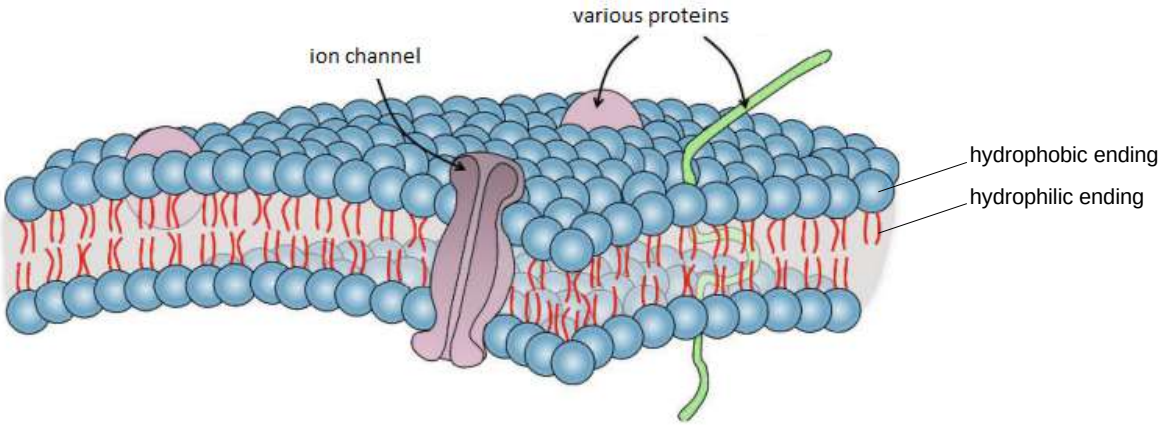

Figure 2: The cell membrane consists of a lipidic bilayer with ion channels, that allow ions to traverse the barrier. Figure taken from Beck et al.[8]

The Na^+/K^+-ATPase is an enzyme, that uses adenosine triphosphate (ATP), the human body's main energy source, to transport 3 Na^+ ions out of the cell and 2 K^+ ions into the cell. It is also referred to as the "*ion pump*". This imbalance of charge results in the formation of an electrical field. If the permeability of one ion is considerably higher than the permeability of the remaining species, then it will dominate the Goldmann equation and the resulting voltage will be close to that ions Nernst voltage.[5] The resting membrane potential of neurons is in the range of -60 mV, which can be accurately fit with the Goldmann equation using the following permeability ratios[4]:

$$P_{K^+}:P_{Na^+}:P_{Cl^-}=1:0.04:0.45$$

Equation 4: Permeability ratios for cell membrane at rest[4]

At the peak of the action potential the membrane is much more permeable to sodium ions, and the membrane potential reaches almost 55 mV, which is the Nernst potential of sodium, and the following permeability ratios more accurately describe the membrane potential in the Goldmann equation:

$$P_{K^+}:P_{Na^+}:P_{Cl^-}=1:20:0.45$$

Equation 5: Permeability ratios for cell membrane at the peak of action potential[4]

By opening or closing ion channels, the cell can change its resting potential. The change in potential is caused by a change in the ion permeabilities as described by the Goldmann equation[4].

6.3 Action potential

A decrease in membrane potential is referred to as hyper-polarisation, if the membrane potential becomes more positive, this is called depolarisation. If the depolarisation reaches a certain threshold value, ion channels start to open up for sodium ions, which further increases depolarisation, which in turn leads to even more ion channels opening. The result is a cascade of channels opening, which causes a strong sudden increase of the membrane voltage. This can be seen in figure 3. The resulting signal is referred to as the action potential. The strength of the action potential is around 100 mV and the duration is about 2 ms. For a short amount of time after activation, the ion channels

are less receptive to stimulation, which is referred to as refractory period. During this period the ion pump restores the initial state.

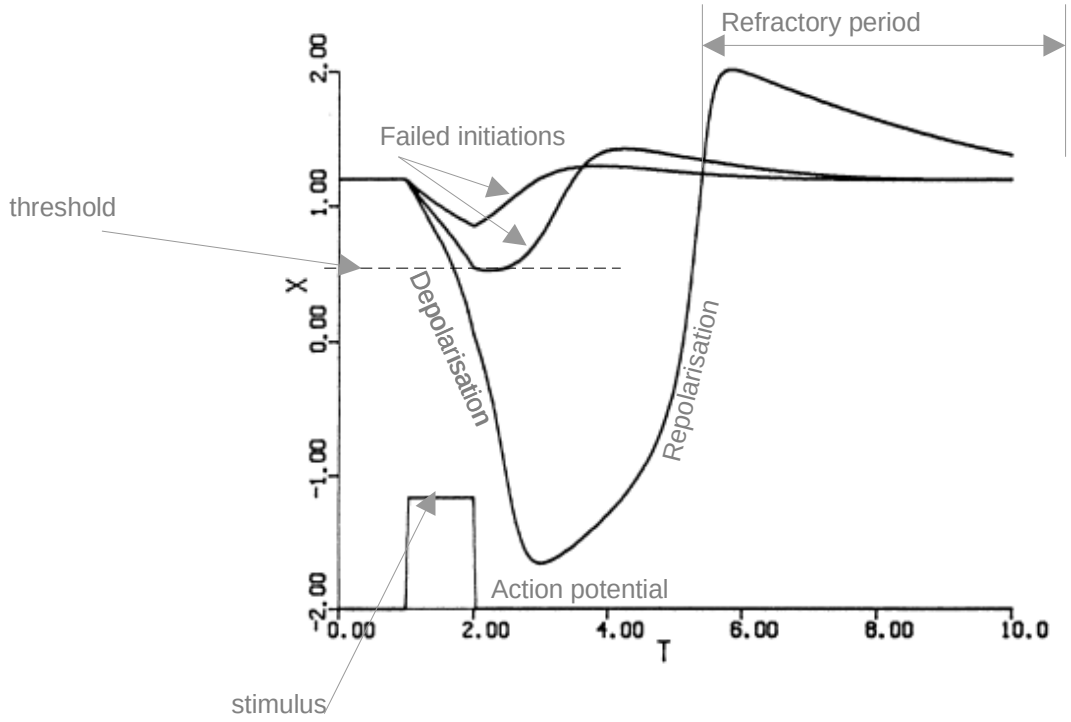

Figure 3: The development of an action potential. Figure adapted from Rattay [11]

6.4 Signal propagation

Figure 4 shows the propagation of the action potential along an unmyelinated cylindrical axon. The depolarisation in the active region spreads towards the neighbouring regions. However, following the depolarisation of the cell membrane, the K^+-channels are mostly open, allowing the potassium ions to balance out this depolarisation. This means, that for a certain period after depolarisation (until the K^+-channels normalise again due to the sodium/potassium pump) the region of the cell membrane is resistant to renewed depolarisation. This results in a one-directional propagation of the action potential.

Most axons have a diameter around 0.2 -20 µm, which leads to a notable electrical resistance, as the ions carrying the charge along the axon collide with many other particles in the cell fluid[4]. To improve the conducting properties, certain axons are covered in a myelinated sheath, which is interrupted at regular intervals by the nodes of Ranvier[6]. The myeline sheath acts as an insulator against the extracellular tissue, facilitating the separation of charge and reducing the leakage of ions. The nodes of Ranvier contain a high density of ion channels, which can open if an action potential above a certain threshold reaches the node, thus allowing for an increased flux in sodium ions and restoring the action potential to its starting intensity[6]. The propagation speed is slowest at the nodes of Ranvier and considerably faster in the myelinated segment, creating the appearance of a “jumping” transmission, which is referred to as “saltatory conduction”[4] (figure 4C).

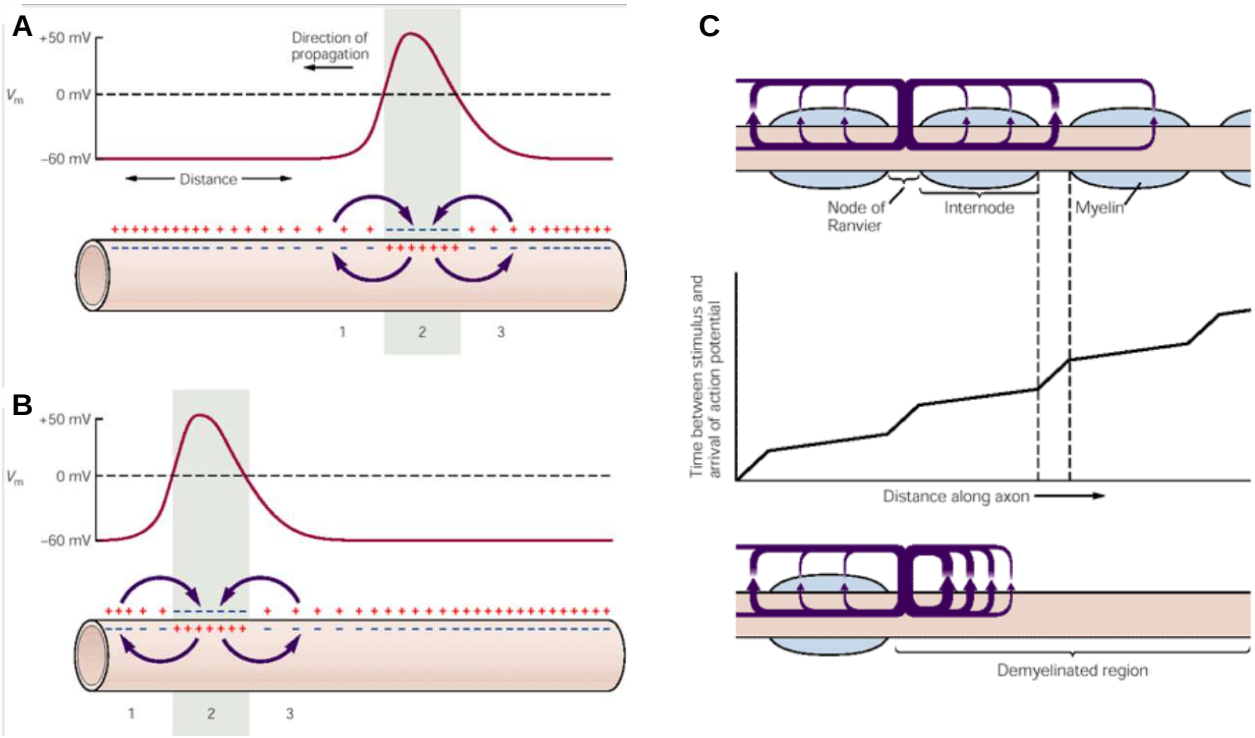

Figure 4: Propagation of the action potential along an axon. A and B show the unmyelinated axon. The depolarisation in the active region (2) spreads towards the neighbouring regions (1) and (3). The currents in A lead to the charge distribution in B, resulting in a net movement of the action potential. C shows the myelinated axon. The speed of conduction is slowest in the nodes of Ranvier. Figure taken from Kandel et al.[4]

6.5 Motor unit

A muscle consists of a large number of muscle fibres. Groups of these are innervated by a single motor neuron. This is referred to as "motor unit", which is shown in figure 5, and consists of the motor neuron and innervated muscle fibres connected via the neuromuscular junction. Because the neuron can only transmit binary all-or-nothing signals, the motor units are the indivisible elements of muscle movement[7]. Depending on the type of muscle and the precision of movement required, the amount of muscle fibres controlled by a single motor neuron can vary from 3 for the eye muscle to 10 000 in leg muscles[8]. The strength of the muscle movement can be gradually controlled, by changing the amount of simultaneous motor units in action and frequency of stimulation.

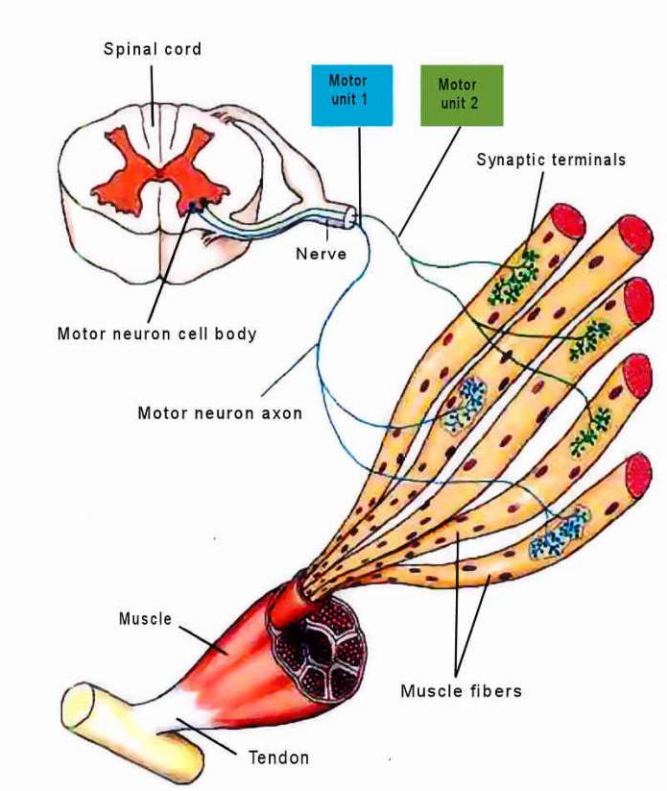

Figure 5: Depiction of a motor unit. Figure taken from Campbell et al. [2]

6.6 Functional electrical stimulation

Functional electrical stimulation (FES) is used, to elicit a muscular response by stimulation via short electrical pulses. The necessary stimulus is presented to the nervous system via electrodes which provide a current pulse[9]. This pulse changes the separation of charge across the cell membrane and therefore the potential. For currents below the excitation threshold of the neuron, the cell membrane can be described by a resistor and a capacitor by the following simplified electrical circuit (figure 6):

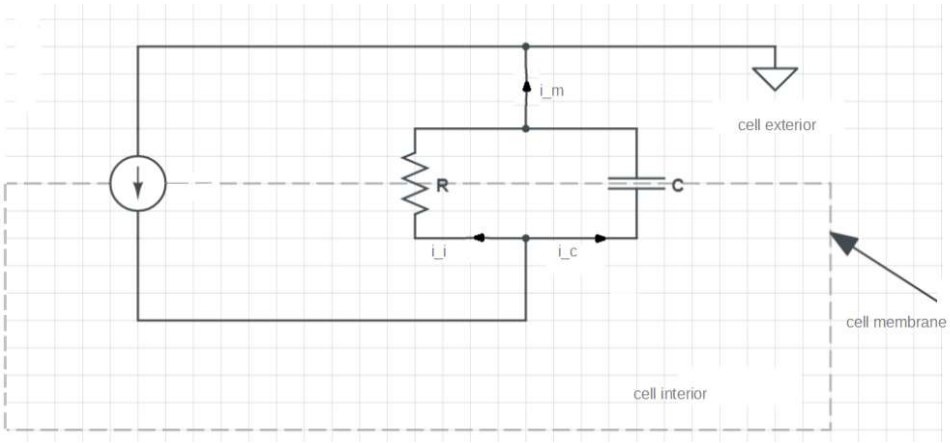

Figure 6: Electrical equivalent circuit of the cell. The cell membrane has resistive as well as capacitive features. Adapted from Kandel et al.[4]

The voltage response to a current pulse can be seen in Figure 7. The capacitive (i_c) and the ionic current (i_i) make up the total current across the membrane (i_m). The total response (figure 7 response 'c') is a combination of a strictly resistive response (figure 7 response 'a') and a strictly capacitive response (figure 7 response 'b'). The time constant describes the necessary time to reach 63% of the maximum response, and it is in the range of 20 – 50 ms for nerve cells[4].

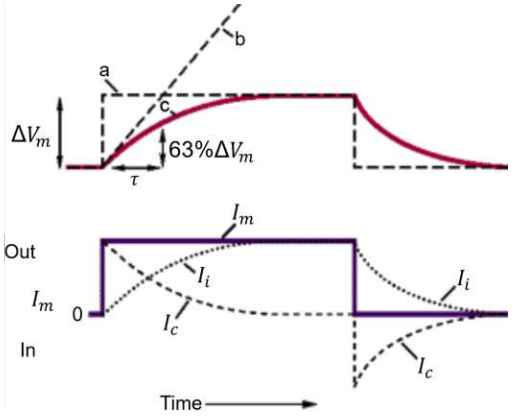

Figure 7: Voltage response to a current pulse across the cell membrane. Figure taken from Kandel et al. [4]

Stimulating pulses predominantly elicit action potentials close to the cathodic electrode.[9] The artificially induced action potential travels in both directions (anterograde and retrograde) along the axon.[10] As the propagation of the AP is an autonomous natural process, the receiving target is unable to differentiate between AP´s of natural or artificial origin. Therefore the return electrode does not need to be placed at the end of the nerve fibre. It is enough, that the current flows through a short part of the nerve, to elicit the full activation of the motor unit.

In order to prevent corrosion of the electrodes and tissue damage, the stimulating pulse must be followed by a charge balancing pulse[11]. Therefore a charge balanced current controlled stimulation is strongly recommended over a voltage controlled stimulation, especially for chronically implanted components.

There are different approaches to the supply of current to the nerve. The least invasive form is via surface electrodes placed on the skin[11]. These electrodes need to overcome the relatively high resistance of the skin and reveal a relatively low fiber selectivity[11]. For a more precise targeting of specific nerves, needle electrodes can be inserted into the proximity of the nerve, or a cuff electrode can be surgically wrapped around the nerve[12]. A cuff electrode can have several contacts, allowing for stimulation from different sides of the nerve, ideally resulting in selective stimulation of different compartments of the nerve[12].

As the nerves reach the periphery of the body, they branch out to innervate individual muscles and organs of the body. Before branching of from the main strand, the nerves group up in fascicles which innervate similar areas of the body, to be nearby. This can be seen in Figure 8A. Figure 8B shows the cross section at a position at which the nerves already separated.

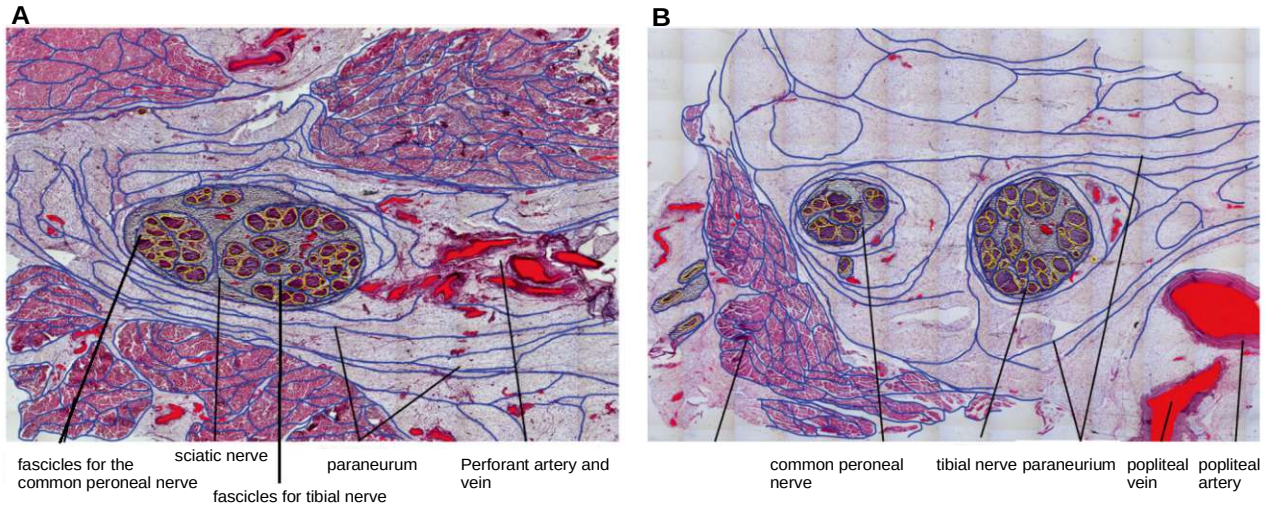

Figure 8: A) Cross section of the human sciatic nerve and surrounding tissue before the common peroneal nerve and the tibial nerve separate. Hematoxylin-eosin stained. B) Cross section of the human sciatic nerve and surrounding tissue after common peroneal nerve and tibial nerve have separated. Hematoxylin-eosin stained. Figures taken from Reina et al.[21]

The precise knowledge of the position of these fascicles is required for selective stimulation of specific muscle groups using multichannel nerve cuff electrodes. Figure 9A shows a schematic placement of a 4-channel cuff electrode. The position of the cuff electrode can be seen in Figure 9B. The proximal direction points towards the central nervous system and the distal direction points towards the periphery of the body. In this particular case, the 90° electrode would preferably stimulate the tibialis nerve, and therefore the attached gastrocnemius muscle while the 270° electrode would preferably stimulate the common peroneal nerve and the attached tibialis anterior muscle.

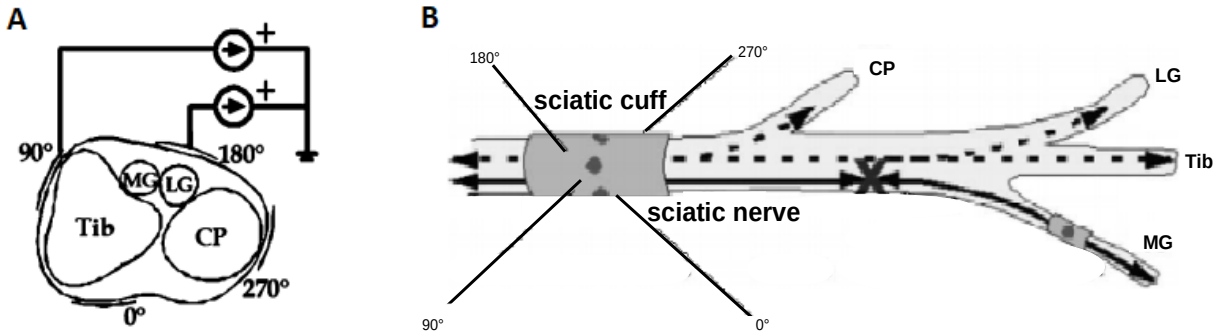

Figure 9: A) Schematic cross section of the sciatic nerve with a cuff electrode with 4 separate electrodes attached to it. The fascicles which form the tibial nerve (Tib) and the common peroneal nerve (CP) are visible as well as the medial gastrocnemius and the lateral gastrocnemius nerve. B) The position of the nerve cuff. One can see the nerve branching point, at which the nerve splits up into the tibial nerve, the medial gastrocnemius and the lateral gastrocnemius. Figures adapted from Tarler et al.[25]

Unfortunately it is not possible to know the configuration of the fascicles prior to dissection, which means, that after implantation of the nerve cuff electrode the nerve reaction on the indiviual channels needs to be assessed through further measurements in each subject separately.

There are several ways to measure the response of the muscle to a stimulus. The most informative is a force measurement of the muscle[9]. This is performed by fixating the muscle and attaching it to a force transducer or by measuring the joint torque. These measurements require the muscle to be isolated from the surrounding tissue and thus require a long surgical preparation, which puts a lot of strain on the test subjects. Generally these measurements are performed in terminal experiments.

A very good alternative to the direct force measurement is the electromyographic (EMG) measurement[13]. Upon receiving a signal from the nerve, a muscle action potential is transmitted down the length of the muscle, which leads to a contraction of the muscle. Each muscle fibre can only react in a binary fashion. A gradual generation of force is possible by varying the amount of active muscle fibers in a muscle and the stimulation frequency. The EMG signal is measured by placing 2 electrodes longitudinally on the skin above muscle (surface electrodes) or into the muscle (needle electrodes)[13]. The evoked signal amplitude is strongly dependant on the position of the electrode and thus it should be generally normalised towards the potential measured at maximum force[13].

The recruitment characteristics of a muscle can be visualised with a recruitment curve. Several recruitment curves at different with pulses of differing stimulation length can be used to generate a strength duration curve (SD curve) and a charge duration curve (CD curve)[14]. Figure 10 shows the typical shape of a strength duration curve. The curve describes the necessary amplitude that a stimulation pulse of the given duration needs, in order to elicit a noticeable muscle contraction. The two relevant parameters to describe the excitability of the cells are the chronaxie and the rheobase. The rheobase describes the minimum amplitude, that a pulse of theoretically infinite length needs, to achieve stimulation. The chronaxie is the pulse duration at a threshold amplitude, that is twice the rheobase. The charge duration curve describes an approximately linear relationship between the pulse duration and the necessary charge to achieve stimulation. The chronaxie and the rheobase allow a quantification and therefore a comparison of the excitability of a neuron.

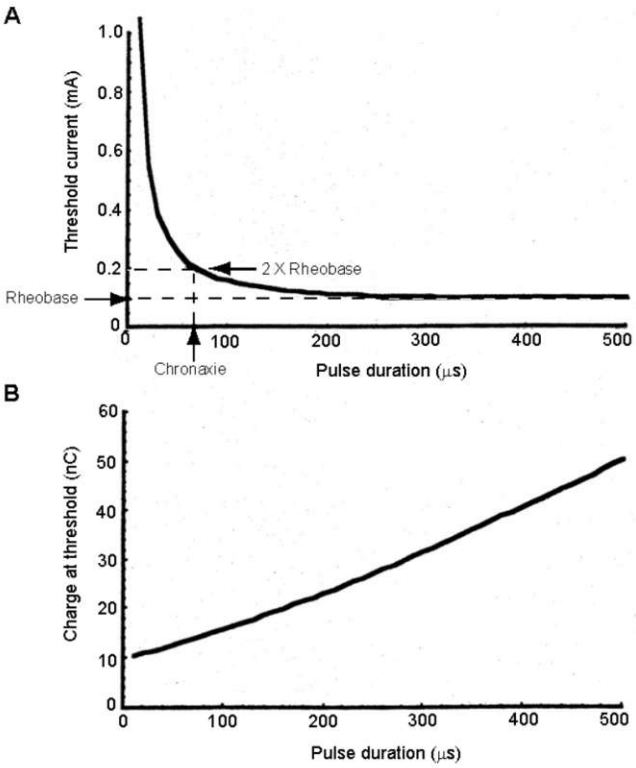

Figure 10: Typical shape of a strength-duration (A) and charge-duration (B) curves. Figure taken from Liu Shi Gan et al.[14]

6.7 Systems for transcutaneous energy transfer

Many implants require an amount of energy which can no longer be supplied by an implanted battery. A total artificial heart requires 8 - 12 W for example[15]. Currently many systems include a percutaneous tube, which protrudes the skin and contains the necessary wiring. However this tube is very often the site of infection, and therefore systems for transcutaneous energy transfer (TET) would be a highly desirable replacement for the percutaneous variant. The TET is able to transfer energy to the implant without breaking the skin barrier. Currently TET systems rely on the inductive coupling of energy between an interior and an exterior coil. The interior coil is shaped like a dome, so that it produces a bulge under the skin and therefore facilitates the alignment of the coils[15]. A regulator circuit was used to convert the high frequency current into a DC current to charge an internal battery. These TET system can provide up to 70 - 80 W[15]. The efficiency of power transfer, which is optimally in the range of 70 - 80%, is strongly dependent on the alignment of the coils and is a very important parameter, as the energy loss produces heat and can damage the surrounding tissue[15].

An alternative for the inductive system was examined by Erfani et al.[16] using capacitive coupling at at frequencies around 150 - 200 MHz. These experiments were performed in an ex vivo environment and required circuit electronics on the receiving end of the coupling array. Erfani et al. studied the effect of misalignment on the transfer efficiency, trying to reduce the energy loss and consequently the heat generation of the array.

Another alternative to the inductive system was proposed in a proof of concept study by Kiele et al.[17] They supplied the implant by directly placing multiple electrode pairs on the skin and transmitting the energy with the skin as intermediate layer[17]. Alignment of the electrodes was achieved by placing strong neodymium magnets at the back of the electrodes. An advantage over the inductive approach was the reduced bulkiness of the implant, as it only consists of thin and flexible structures. This should reduce the risk of pressure sores and skin irritations[17]. Additionally the system by Kiele et al. would not require any internal circuit board for the transformation of AC current. The simplicity of this system was expected to be more robust and better accepted by the surrounding tissue, thus leading to a longer functional lifetime[17]. The experiments in the proof of concept study by Kiele et al. were performed on a human tissue sample.

7 Objectives

Current systems to stimulate nerves include fully implanted designs[18] as well as designs using inductive coupling to transfer the energy and the signal through the skin[19] and designs utilising surface electrodes. Some muscles are very difficult to stimulate selectively using surface electrodes, as other groups of unintended fibres are often stimulated as well[11]. Fully implanted systems on the other hand can be applied directly onto the desired nerve. One disadvantage of many fully implantable systems is the dependence on the lifetime of the battery[15]. The inductive systems require implanted electronic circuits to transform the high frequency AC currents into DC signals, which are necessary to evoke a neural response from the nerve[15]. Experiments with purely capacitive coupling have been performed by Erfani et al.[16] at frequencies around 150-200 MHz. These frequencies are too high to directly stimulate the nerve and therefore would also require additional electronics implanted under the skin to transform the signal. Trying to overcome these downsides, we performed experiments with a resistive design based on the proof of concept study by Kiele et al.[17] which allowed to externalize all processing electronics. The design by Kiele et al. was less bulky than other TET systems, as it consisted only of thin and flexible structures. The stimulating signal as well as the energy to power the implant would be transferred directly from the receiving internal electrode array to a multi-channel nerve cuff electrode. This proof of concept study was performed on a human tissue sample.

The main objective of this thesis was to test the implementation of the system developed by Kiele et al. in an *in vivo* environment, more specifically female Sprague Dawley rats. The electrode array was placed on the rats back, while the multi-channel nerve cuff electrode was wrapped around the sciatic nerve to produce selective reactions of the gastrocnemius and the tibialis anterior muscles. A percutaneous socket was introduced at the rats head and mounted on top of the skull to allow for direct contact with the implanted components. The physical strain of the implant put on the animal, as well as the mechanical strain the animal put on the implant were to be evaluated. The selectivity of the entire system as well as the individual selectivity of the components, i.e. electrode array and multi-channel nerve cuff electrode, were to be assessed. A crosstalk coefficient of the array was determined by the current distribution of the receiving internal array and the selectivity of the cuff electrode was determined through analysis of the resulting EMG signal in the gastrocnemius and the tibialis anterior muscles. The performance of each separate component was observed and documented in order to improve future designs.

8 Materials and methods

8.1 Animals

The experiments were conducted on 10 female Sprague Dawley rats. The age of the animals was 12 weeks at the time of surgery. Preliminary measurements were performed on 6 additional rats to establish an optimal experiment design. The experiments were performed according to the approved ethics proposal at the Austrian ministry of science under the proposal number: *2020-0.363.116*

All experiments were performed according to the FELASA guidelines[20].

8.2 Experimental setup

A schematic of the entire experimental setup can be seen in figure 11. A stimulator was used to send current through the skin via the electrode array. The signal from the external array was picked up by the implanted internal array and transferred to the headstage. The electrodes of the array were aligned and held in place by strong neodymium magnets. In the headstage, the output of the internal array was connected with the input of the nerve cuff electrode via a jumper cable. Alternatively, the pins of the headstage socket could be accessed directly to contact all components separately. The nerve cuff electrode applied the stimulation current to the sciatic nerve and thus evoked contractions of the gastrocnemius and the tibialis anterior muscles. The EMG of these contractions was measured using needle electrodes which were inserted into the muscle. The ground electrode was a surface electrode placed on the palm of the leg which was not stimulated. Alternatively the nerve cuff electrode also had an internal ground electrode which could be contacted via the headstage socket. The implant was designed and developed by the Laboratory for Biomedical Microtechnology, Department of Microsystems Engineering (IMTEK), University of Freiburg, Germany.

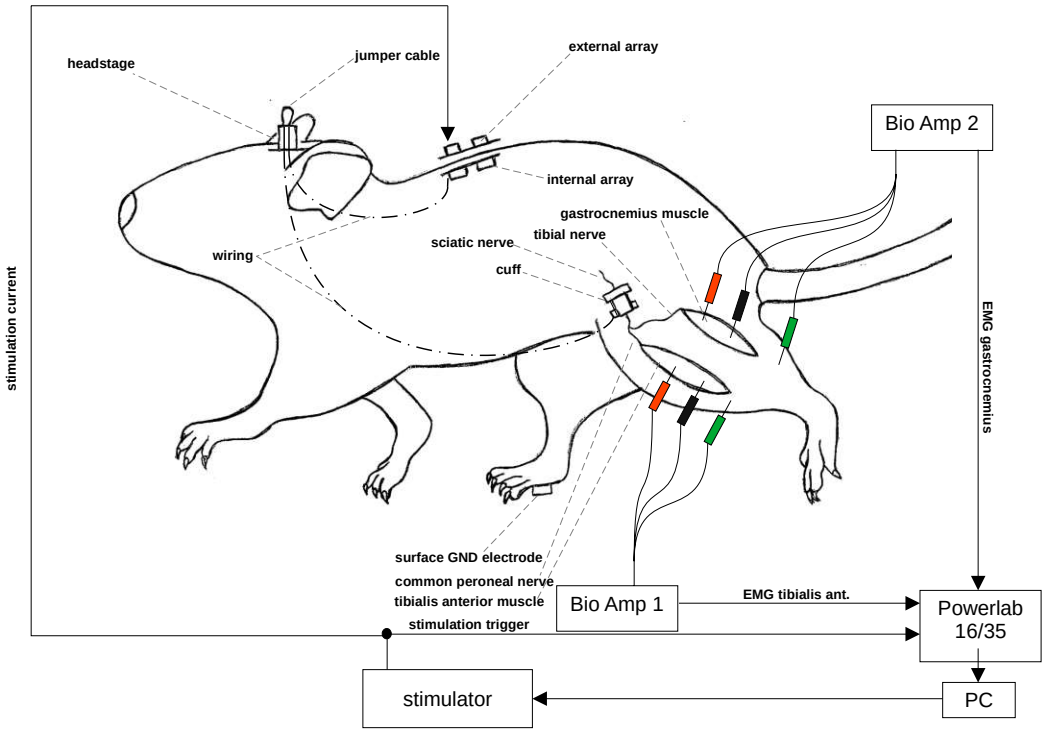

Figure 11: Schematic overview of the system and its components. The system consists of a coupling array on the animals back, a multi channel cuff electrode wrapped around the sciatic nerve as well as a headstage socket protruding the skin on the top of the head.

Figure 12 shows the layout of the electrodes on the transfer array. The diameter of the electrodes on the internal array was 5 mm while the electrodes on the external array had a diameter of 6 mm. This difference in size reduced misalignment. The center-to-center pitch of the electrodes is 15 mm. Neodymium magnets were located at the back of each electrode to ensure proper alignment.

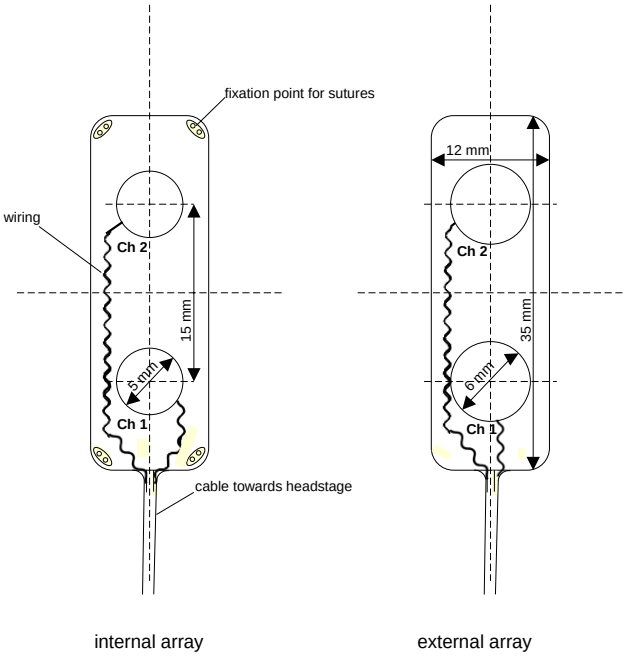

Figure 12: Layout of the electrodes on the transfer array. Neodymium magnets are located at the back of each electrode to ensure proper alignment.

8.3 Surgical procedure

The surgical procedure was performed under anaesthesia by a trained medical professional. A skin incision 1-2 cm long was made on the top of the head and a subcutaneous canal was tunnelled to a second ~4 cm long incision in an imaginary line between hip and knee. The cable to the cuff electrode was passed through this tunnel. The sciatic nerve was located between the gluteus superficialis muscle and the biceps femoris muscle and was carefully freed over a length of approximately 2 cm before it split into its two terminal branches. The cuff electrode was positioned at the mid-level of the sciatic nerve before it branched. After the nerve had been exposed, the electrode was placed around the nerve and fixed with two 6-0 Ethilon single button sutures. Figure 13c shows the nerve cuff electrode wrapped around the sciatic nerve. To connect the implanted cables to the extra-corporeal stimulator/recorder during the measurements, a headstage socket (figure 13a) was attached to the head with bone cement and a screw to the skull. The cap of the headstage was the only component protruding through the skin and it allowed to contact the wiring of the implant as soon as the protective cap was removed. To position the internal array, an additional ~3 cm long incision was made on the back of the animal and a subcutaneous pocket was prepared. From here a subcutaneous tunnel was created to the head-stage. Figure 13 shows an implant with 4 electrodes. This was the prototype used in the preliminary measurements. The version used in the main experiments was a shorter version of the same implant containing only two electrodes.

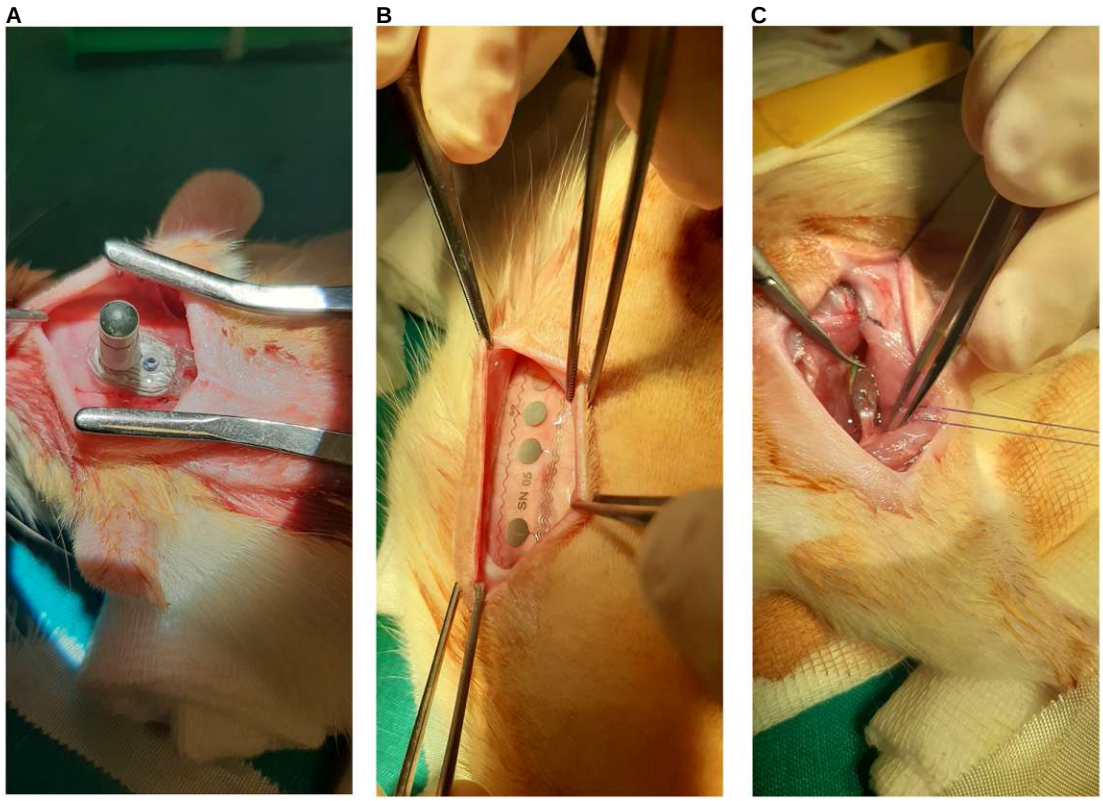

Figure 13: A) shows the headstage socket. The cap can be removed to access the internal wiring below.): shows the implanted part of the array on the animals back. C) shows the hind leg and the nerve cuff electrode wrapped around the sciatic nerve.

8.4 Preliminary measurements

Before the main experiments preliminary pilot experiments were performed to optimize the experiment protocol. These measurements had an impact on the implant design and the measurement protocol. The main parameters which we aimed on improving were the mechanical durability, the signal quality and the duration of the measurement.

8.5 Measurement protocol

8.5.1 Impedance measurement

Impedance measurements were primarily performed to gather information on the condition of the implant. The *EIMS- Multichannel system* (Ottobock SE & Co. KGaA, custom made, Vienna, Austria) with a data acquisition system (*NI DAQ: USB 6225*, National Instruments, Austin, Texas) was used to measure the resistance at varying frequency in a range between 10 Hz-10kHz (i.e. 10, 20, 40, 60, 80, 100, 200, 400, 600, 1000, 2000, 4000, 6000, 8000, 10000 Hz). The measurement current was 500 nA. Prior to measurement a calibration was performed using resistors of known value (3.9 kΩ and 1.5 MΩ). Unusually high impedances would indicate wire breakage. The impedances were measured at several positions to better localize potential problems. Table 2 shows a list of the impedances which were measured. The positions of the electrodes for the impedance measurement can be found in figures 14 and 15. The impedances were measured between the external and the internal array (figure 14A), between each channel of the cuff electrode and the internal ground electrode of the cuff (figure 14B), between each channel of the external array as well as the internal array and the surface ground electrode (figure 15A) and between each of the channel of the cuff electrode and the surface ground electrode (figure 15B). All electrodes of the external array were coated with a small amount electrode-gel to improve the coupling properties.

Impedances Measured

External Array	-	Internal Array	Fig. 14A
Cuff channel	-	Cuff ground	Fig. 14B
External Array	-	Surface Ground	Fig. 15A
Internal Array	-	Surface Ground	Fig. 15A
Cuff channel	-	Surface Ground	Fig. 15B

Table 2: Overview of the impedances measured

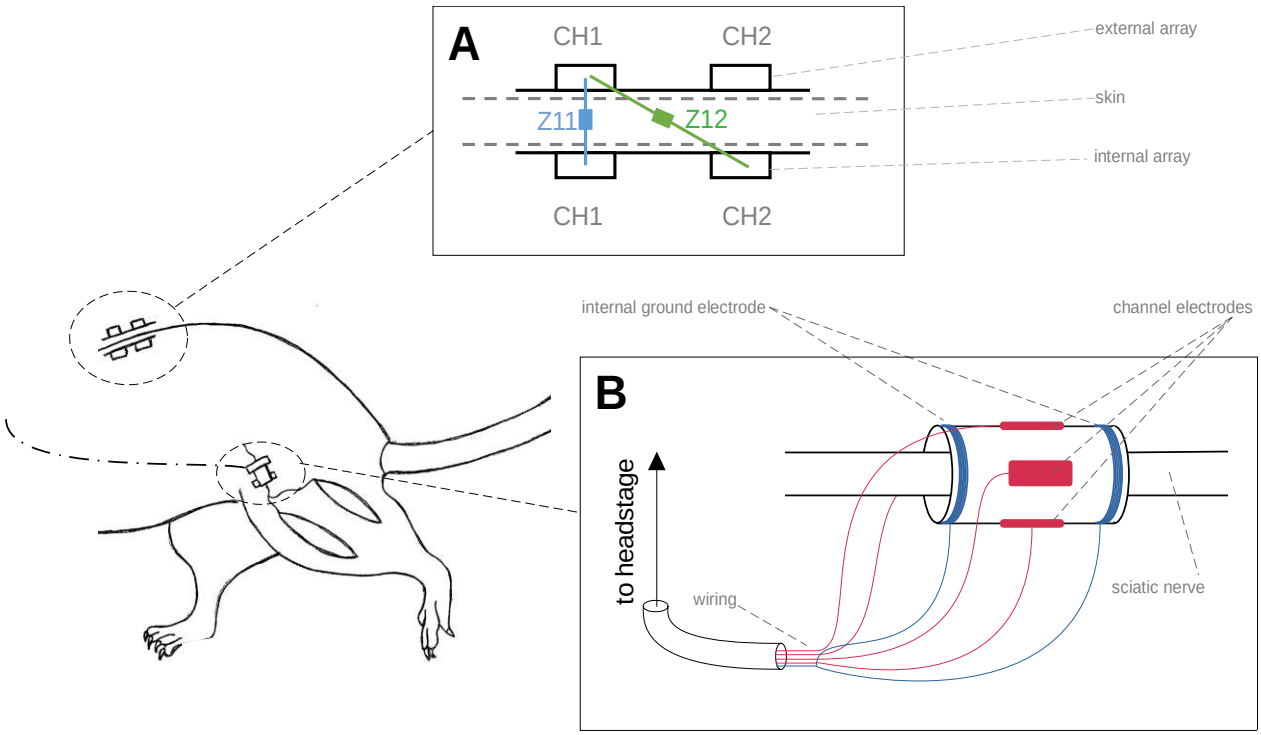

Figure 14: the figure shows a detailed view of the electrode configuration during the experiments. A) shows a detailed view of the array and the impedances measured. B) shows a detailed view of the cuff electrode. The impedances were measured between each of the channel electrodes and the internal ground electrode.

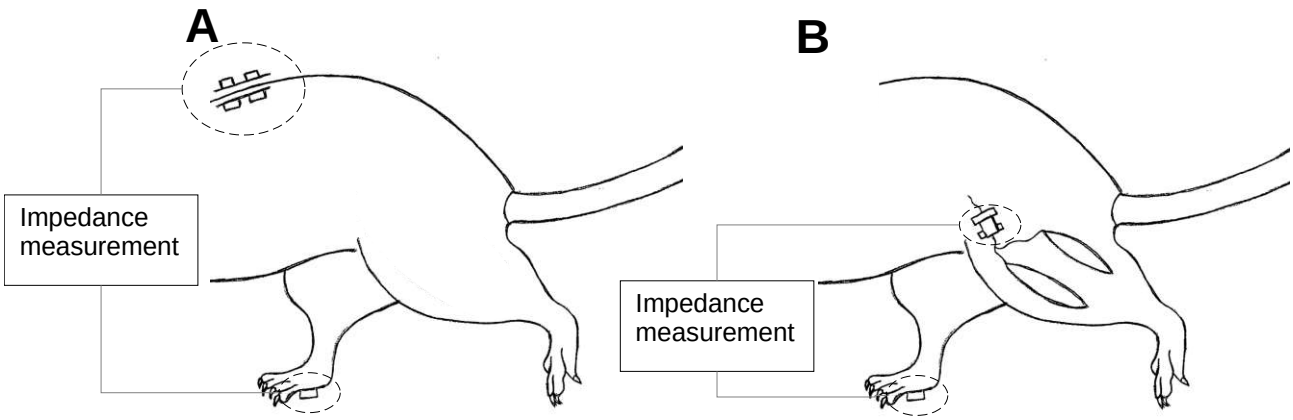

Figure 15: A) Impedance was measured between the external array electrodes and the surface ground electrode as well as between the internal array electrodes and the surface ground electrode. B) Impedance was measured between the channels of the cuff electrode and the surface ground electrode, which was attached to the other foot.

8.5.2 Stimulation parameters

Table 3 contains an overview of the stimulation parameters for all experiments performed. Two different stimulators were used for the experiments. The CorTec stimulator (*CorTec BIC evaluation kit, CorTec GmbH, Freiburg, Germany*) allowed for stimulation with shorter phase widths, thus allowing for a more precise recruitment during the measurement of the nerve cuff properties.

Unfortunately the compliance voltage of the CorTec stimulator of U_{comp}= 11 V was not high enough to overcome the resistance of the skin. Therefore it was only used for the cuff measurements. The Isis stimulator (*Inomed Medizintechnik GmbH, Emmendingen, Germany*), which had a higher compliance voltage (U_{comp}= 410 V), was used for the experiments as well. Experiments involving sending current through the skin were only performed with the Isis stimulator.

Stimulation Parameters

Experiment type	Stimulator	Amplitude range [µA]	Phasewidths [µs]
Coupling parameters	Isis	500 - 5000 : 500*	50,100,500,1000
Selectivity cuff(CorTec)	CorTec	48- 960 : 48; 1056 – 1920 : 96	10,100,500,1000
Selectivity cuff(Isis)	Isis	100 – 1000 : 100	50,100,500,1000
Selectivity cuff + surface GND	Isis	100- 1000 : 100	50,100,500,1000
Evaluation of full system	Isis	100 – 5000 : 100	50,100,500,1000

Table 3: Stimulation parameters of all different experiments. The following format is used: "lower limit – upper limit : stepsize"

The shape of the stimulation pulses for the different stimulators can be seen in Figure 16. The balance of charge was important to prevent corrosion of the electrode and damage to the surrounding tissue.

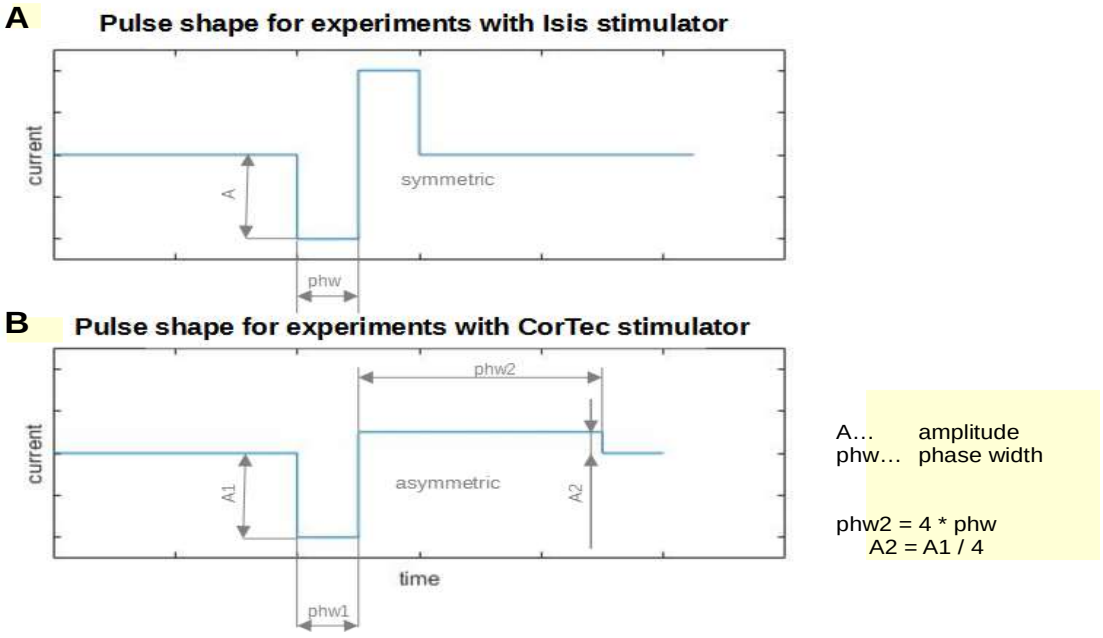

Figure 16: A) shows the shape of the stimulation pulse using the Isis stimulator. The charge balancing phase had the same amplitude and phase width as the stimulating negative phase. B) shows the shape of the stimulation pulse using the CorTec stimulator. The balancing pulse had 4 times the length and one quarter of the amplitude of the stimulating negative phase.

8.5.3 Measurement of coupling properties

The coupling properties of the array were assessed by measuring the current pulses transmitted across the interface between external and internal array individually for each channel (as shown in

figure 17). The Isis Neurostimulator (*Inomed Medizintechnik GmbH, Emmendingen, Germany*) was set to produce short bursts of symmetric biphasic pulses (frequency 70 Hz, burst duration 500 ms, pulse shape is shown in figure 16a) with the parameters specified in table 3 through a custom written Labview script (*LabVIEW NXG 5.1, National Instruments, Austin, Texas*)provided by the company. The stimulation amplitude was varied from 0.5 mA to 5 mA in 0.5 mA steps for different phase widths (i.e. 50, 50, 100, 500 µs). The current was determined by recording the voltage drop over a resistor (10 Ω) using a Powerlab data acquisition system (*PL 3516 Powerlab 16/35, ADInstruments, Dunedin, New Zealand*) at a sampling frequency of 100 kHz and saved as a Matlab file using Labchart software (Labchart v. 8.1.16, *ADInstruments, Dunedin, New Zealand*). Each channel was connected to a total load of 2.2 kΩ (of which 10 Ω were the resistor over which the voltage drop was measured) to the ground of the stimulator. Figure 17 shows the position of the resistors in this experimental setup. The current splits up between the channels 1 and 2 while it passes through the skin. A selective array should have a negligible amount of crosstalk current.

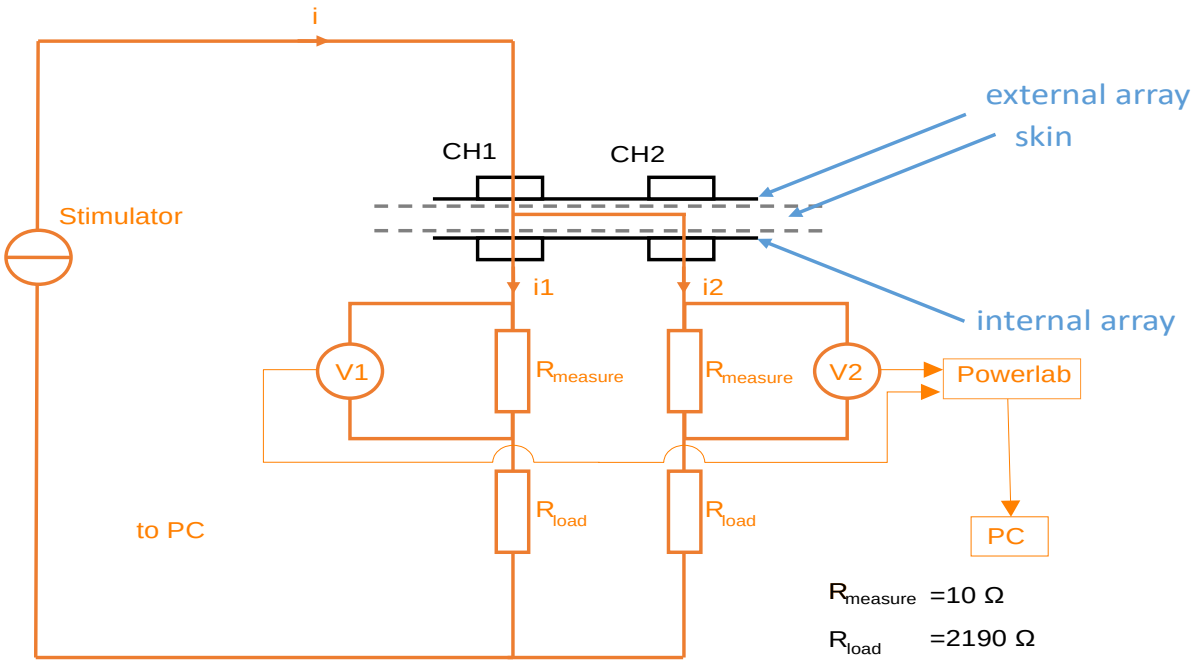

Figure 17: The current split up between channels 1 and 2. These currents were measured over 2 resistors (10 Ω) using the Powerlab 16/35 and saved to the PC. In this case CH1 is the selected input channel and the current "i2" is the crosstalk current. A selective array would have a negligible amount of crosstalk current on i2.

8.5.4 Measurements of cuff selectivity

These measurements focused on the determination of the selectivity of the cuff electrode wrapped around the sciatic nerve. The selectivity describes the percentage of achievable activation in one muscle before another muscle reaches its activation thresholds and starts to contract. A high selectivity (close to 100%) in favour of the gastrocnemius would therefore mean, that the gastrocnemius muscle could be almost entirely activated without the tibialis anterior muscle interfering. The selectivity was measured using three different setups:

Cuff (CorTec-Stimulator)

Measurements were performed using the CorTec stimulator (*CorTec BIC evaluation kit, CorTec GmbH, Freiburg, Germany*). The stimulator was directly connected to the individual channels of the nerve cuff electrode via the headstage, providing biphasic, rectangular current pulses with an asymmetric charge compensation which had 4 times the length and one quarter of the amplitude of the stimulation pulse (see table 3, figure 16b). The internal ground electrode of the cuff was used as anode while one of the 4 channels served as cathode. A series of current pulses separated by 1 s was applied automatically through acustom python script (provided by the company), varying the stimulation amplitude (i.e. 48-960 µA in 48 µA steps and 1056-1920 µA in 96 µA steps) for different phase widths (i.e. 10, 50, 100, 1000 µs). The evoked EMG responses of the tibialis anterior and the gastrocnemius muscles were recorded along with the stimulation pulse over a 100 Ω resistor using a Powerlab 16/35 (ADInstruments, Dunedin, New Zealand) with two connected biosignal amplifiers (BioAmp FE231, ADInstruments, Dunedin, New Zealand) at a sampling frequency of 100 kHz. The data acquisition system was controlled by the manufacturer's Labchart software (Labchart v. 8.1.16, ADInstruments, Dunedin, New Zealand) which further allowed to export data as a matlab file. EMG was recorded via two needle electrodes inserted percutaneously into the muscle while a third needle electrode, serving as reference, was inserted into nearby tissue. Figure 18 shows a schematic illustration of the setup.

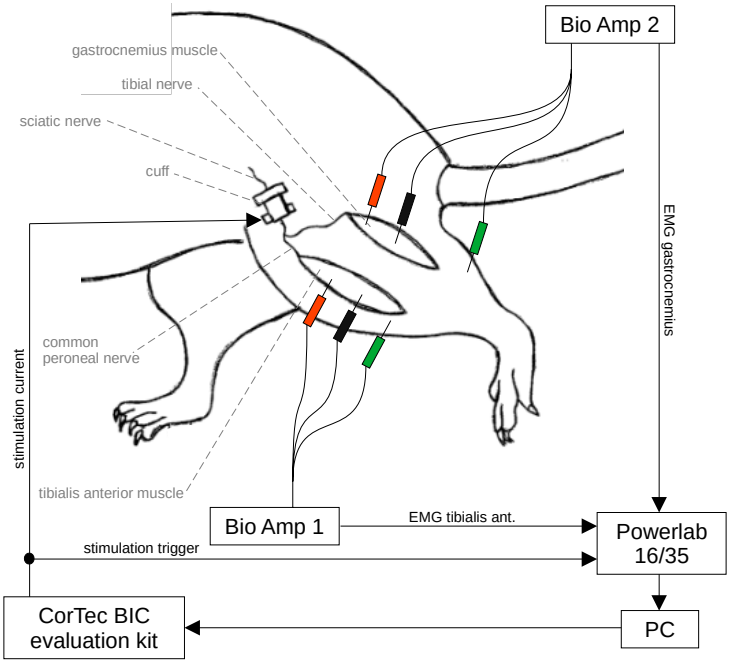

Figure 18: The CorTec stimulator was controlled by a PC and delivered stimulation pulses to the cuff wrapped around the sciatic nerve and a trigger signal to the Powerlab DAQ system. The compound muscle potential was measured by the needle electrodes over a 100 Ω resistor and amplified by the two bioamplifiers. A third electrode was inserted into the nearby tissue to serve as reference.

Cuff (ISIS Stimulator)

These measurements were performed using the Isis Neurostimulator (*Inomed Medizintechnik GmbH, Emmendingen, Germany*). The stimulator was directly connected to the individual channels of the nerve cuff electrode via the headstage, providing biphasic, rectangular current pulses with symmetric charge compensation (see table 3, figure 16a). The input pins of the first and second channel of the cuff electrode were connected. The same was done for the third and fourth channel. This was done to align the amount of electrodes in the cuff with the amount of electrodes in the array. The internal ground electrode of the cuff was used as anode while one of the cuff channels (CH1+CH2 or CH3+CH4) served as cathode. A series of current pulses was applied automatically through a Labview script (*LabVIEW NXG 5.1, National Instruments, Austin, Texas*) provided by the Laboratory for Biomedical Microtechnology, Department of Microsystems Engineering (IMTEK), University of Freiburg, Germany. varying the stimulation amplitude (i.e. 100 -1000 µA in 100 µA steps) for different phase widths (i.e. 50, 100, 500, 1000 µs). The evoked EMG response of the tibialis anterior and the gastrocnemius muscles were recorded along with a trigger signal using a Powerlab 16/35 (ADInstruments, Dunedin, New Zealand) with two connected biosignal amplifiers (BioAmp FE231, ADInstruments, Dunedin, New Zealand) at a sampling frequency of 100 kHz. The data acquisition system was controlled by the manufacturer's Labchart software (Labchart v. 8.1.16, ADInstruments, Dunedin, New Zealand) which further allowed to export data as a matlab file. EMG was recorded via two needle electrodes inserted percutaneously into the muscle while a third needle electrode, serving as reference, was inserted into nearby tissue. Figure 19 shows a schematic illustration of the setup.

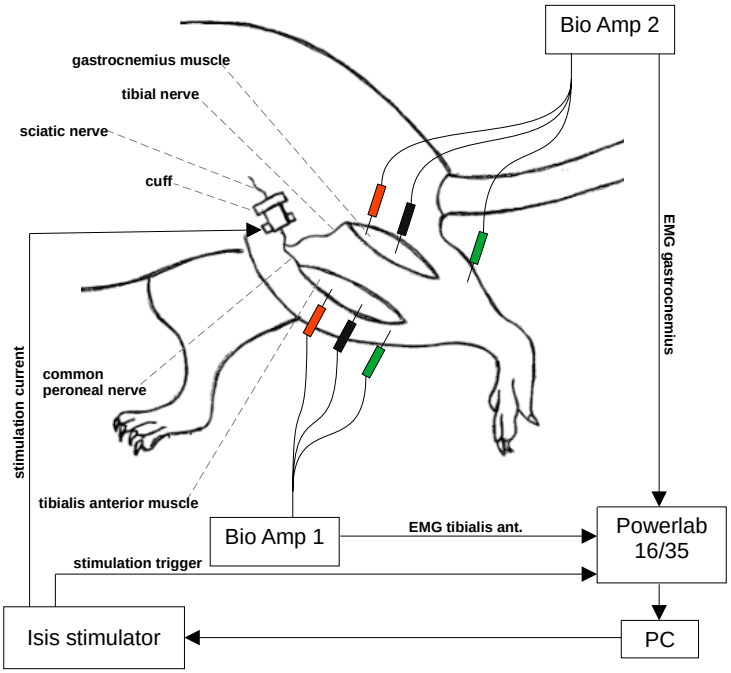

Figure 19: The Isis stimulator was controlled by the PC and sent stimulation pulses to the cuff wrapped around the sciatic nerve and a trigger signal to the Powerlab DAQ system. The compound muscle potential was measured by the needle electrodes and amplified by the two bio amplifiers. A third electrode was inserted into the nearby tissue to serve as reference.

Cuff + surface ground (ISIS- stimulator)

These measurements were performed using the Isis Neurostimulator (*Inomed Medizintechnik GmbH, Emmendingen, Germany*). The stimulator was directly connected to the individual channels of the nerve cuff electrode via the headstage, providing biphasic, rectangular current pulses with symmetric charge compensation (see table 3, figure 16a). The input pins of the first and second channel of the cuff electrode were connected. The same was done for the third and fourth channel. This was done to align the amount of electrodes in the cuff with the amount of electrodes in the array. The ground electrode was placed on the palm of the leg which was not stimulated to serve as anode while one of the cuff channels (CH1+CH2 or CH3+CH4) served as cathode. The current flowed partly through the rats body from the cuff channel electrode to the surface ground electrode. The current also flowed through the sciatic nerve leading to a stimulation of the nerve and the attached muscles. A series of current pulses was applied automatically through Labview script (*LabVIEW NXG 5.1, National Instruments, Austin, Texas*) provided by the company, varying the stimulation amplitude (i.e. 100-1000 µA in 100 µA steps) for different phase widths (i.e. 50, 100, 500, 1000 µs). The evoked EMG response of the tibialis anterior and the gastrocnemius muscles were recorded along with a trigger signal using a Powerlab 16/35 (ADInstruments, Dunedin, New Zealand) with two connected biosignal amplifiers (BioAmp FE231, ADInstruments, Dunedin, New Zealand) at a sampling frequency of 100 kHz. The data acquisition system was controlled by the manufacturer's Labchart software (Labchart v. 8.1.16, ADInstruments, Dunedin, New Zealand) which further allowed to export data in as a matlab file. EMG was recorded via two needle electrodes inserted percutaneously into the muscle while a third needle electrode, serving as reference, was inserted into nearby tissue. Figure 20 shows a schematic illustration of the setup.

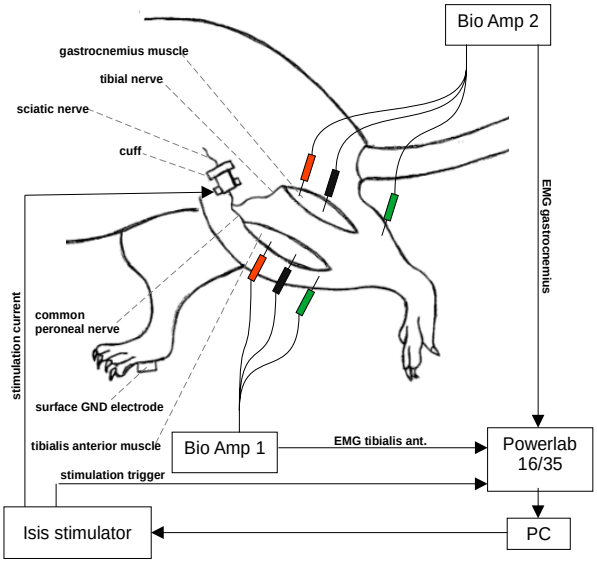

Figure 20: The Isis stimulator was controlled by the PC and sent stimulation pulses to the cuff wrapped around the sciatic nerve and a trigger signal to the Powerlab DAQ system. The compound muscle potential was measured by the needle electrodes and amplified by the two bio amplifiers. A third electrode was inserted into the nearby tissue to serve as reference. The ground electrode for the stimulation current was on the palm of the rats foot. The current flowed through the rats body from the cuff channel electrode to the surface ground electrode. It flowed partly though the sciatic nerve leading to a stimulation of the nerve and the attached muscles.

8.5.5 Evaluation of the full system

The full system consisted of the transfer array directly connected to the nerve cuff electrode via a jumper cable in the headstage. This was the form of the system which may be used in future applications. The measurements were performed using the Isis Neurostimulator (*Inomed Medizintechnik GmbH, Emmendingen, Germany*). The stimulator was connected to the individual channels of the electrode array. Using a jumper cable in the headstage, the output of the internal array was connected to the input of the cuff electrode. The stimulator provided biphasic, rectangular current pulses with symmetric charge compensation (see table 3, figure 16a). The input pins of the first and second channel of the cuff electrode were connected. The same was done for the third and fourth channel. This was done to align the amount of electrodes in the cuff with the amount of electrodes in the array. The ground electrode was placed on the palm of the leg which was not stimulated, to serve as anode while one of the cuff channels (CH1+CH2 or CH3+CH4) served as cathode. The current flowed partly through the rats body from the cuff channel electrode to the surface ground electrode. The current lead to stimulation of the nerve thus activating the attached muscles. A series of current pulses (50 pulses in total, every 500 ms), was applied automatically through a Labview script (*LabVIEW NXG 5.1, National Instruments, Austin, Texas*) provided by the company, varying the stimulation amplitude, i.e. 100-5000 µA in 100 µA, at a phase width of 50 µs. The evoked EMG responses of the tibialis anterior and the gastrocnemius muscles were recorded along with a trigger signal using a Powerlab 16/35 (ADInstruments, Dunedin, New Zealand) with two connected biosignal amplifiers (BioAmp FE231, ADInstruments, Dunedin, New Zealand) at a sampling frequency of 100 kHz. The data acquisition system was controlled by the manufacturer's Labchart software (Labchart v. 8.1.16, ADInstruments, Dunedin, New Zealand) which further allowed to export data as a matlab file. EMG was recorded via two needle electrodes inserted percutaneously into the muscle while a third needle electrode, serving as reference, was inserted into nearby tissue. Figure 21 shows a schematic illustration of the setup. The Isis stimulator had a higher compliance voltage compared to the CorTec stimulator and was necessary to overcome the skins impedance.

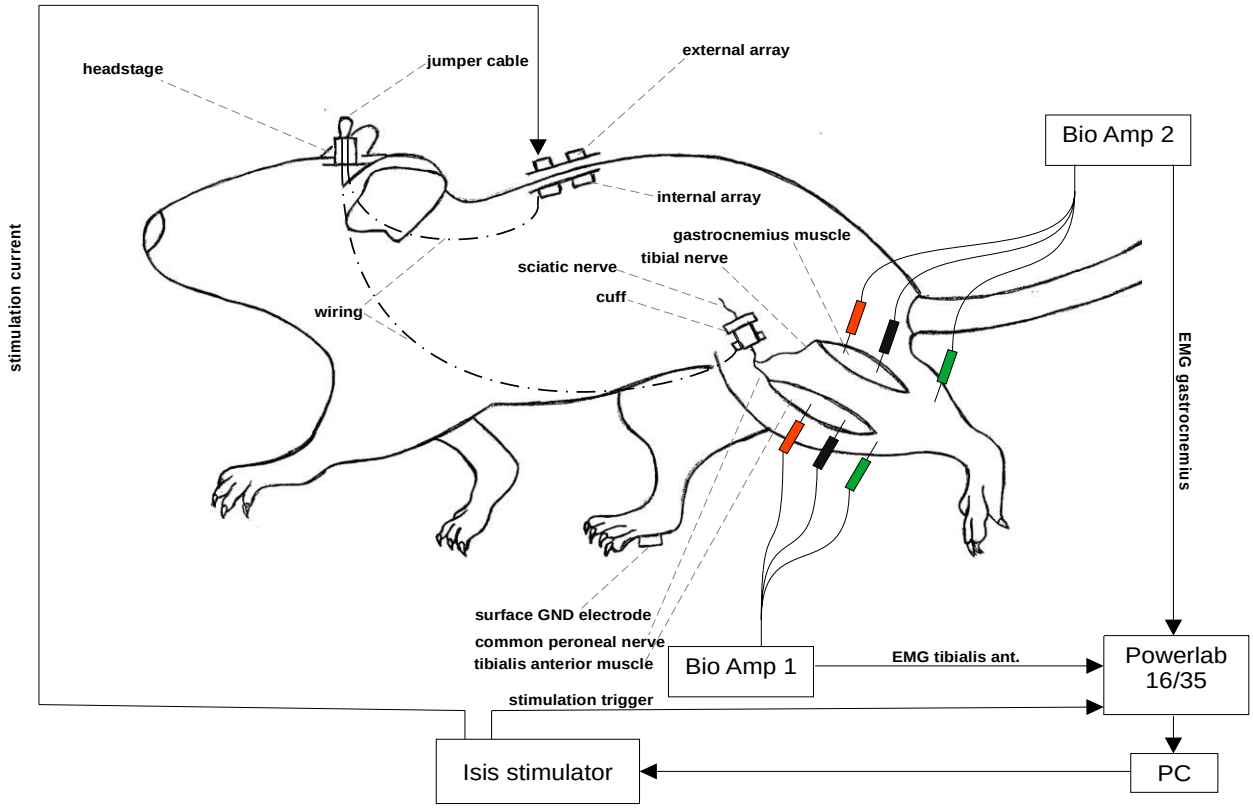

Figure 21: The Isis stimulator was controlled by the PC and sent a trigger signal to the Powerlab DAQ system and stimulation pulses to the external array, which transferred the signal through the skin to the internal array. In the headstage the output pins of the internal array were connected to the input pins of the cuff electrode using a jumper cable. The cuff was wrapped around the sciatic nerve. The compound muscle potential was measured by the needle electrodes and amplified by the two bio amplifiers. A third electrode was inserted into the nearby tissue to serve as reference. The ground electrode for the stimulation current was on the palm of the rats foot.

8.5.6 Experimental schedule

The planed schedule of experiments spanned over 12 weeks after the surgery for each animal. To reduce the amount of strain on the animal on the day of the surgery, only the selectivity measurements using the CorTec stimulator were performed. After the 2nd, 6th, 10th, and 12th week the full set of measurements was performed.

8.6 Data analysis

8.6.1 Analysis of implant lifetime

The impedance measurements were used to determine the first wire breakage or mechanical failure in the system. Due to the temporal spacing of the measurements, the exact time of wire failure could not be determined. The first instance of wire failure in an experiment was taken to estimate the functional lifetime of the implant. These measurements were helpful for the further interpretation of the data and made documentation easier.

8.6.2 Analysis of coupling properties, crosstalk coefficient

The "*crosstalk coefficient*" was defined as a percentage of crosstalk current on the secondary channel in relation to the current received on the primary channel. The channel which is the intended recipient is referred to as "*primary channel*" and the other channel is the "*secondary channel*". This value will further be used to describe the performance of the array.

Figure 22 shows an example of the data obtained from the measurements of the coupling array. In the first column of the figure all 35 peaks can be seen, while the second column shows the zoomed in view, on a single peak of this series. A clear difference is visible in the shape of the short peak and the long peak. The short pulses deviate from the intended rectangular shape. To provide comparable results for the different pulse shapes, each peak was represented by its root mean square (RMS) value. The values used to create this RMS-value are marked in red in figure 22. The negative part of the peak is the stimulation pulse and the positive part is the charge balancing pulse. Only the negative part was used for further analysis. The algorithm to find the peaks defined a threshold value by selecting the highest absolute value in a long period (0.3 s, corresponding to 30 000 data points) without any signal, which consisted only of background noise. As the Labchart script used for data acquisition used a trigger, the signals were exactly at the same position for experiments with different amplitude, as long as the phase width was the same. Therefore we determined the position of the peaks in an experiment with a rather high stimulation amplitude using the previously determined threshold. This allowed us to determine the data point indices in an experiment with high amplitude and use them to define the peaks at all other amplitudes. The high stimulation amplitude was important to guarantee a favorable signal-to-noise ratio which allowed for a clear separation of the signal from the noise. This algorithm was robust in respect to low signal-to-noise ratios and did not produce unexpected errors. The entire burst was then represented as the mean and SD of all the peaks in the burst. Comparing these values on the two separate channels we could determine the current distribution. The current distribution was determined as a percentage of the input current (always totalling to 100% across all channels due to conservation of charge). The crosstalk coefficient is the percentage of crosstalk current on the secondary channel in relation to the current received on the primary channel. A higher crosstalk coefficient signifies a worse performance and at a crosstalk coefficient of 100% the current is split evenly between primary and secondary channel. At values above 100% the secondary channel receives more current than the intended channel. Ideally the crosstalk coefficient should be zero, which would mean, that the entire input current follows the intended path.

$$\text{crosstalk coeff} .= \frac{\text{current}_{\textit{secondary channel}}}{\text{current}_{\textit{primary channel}}}$$

Equation 6: Definition of the crosstalk coefficient

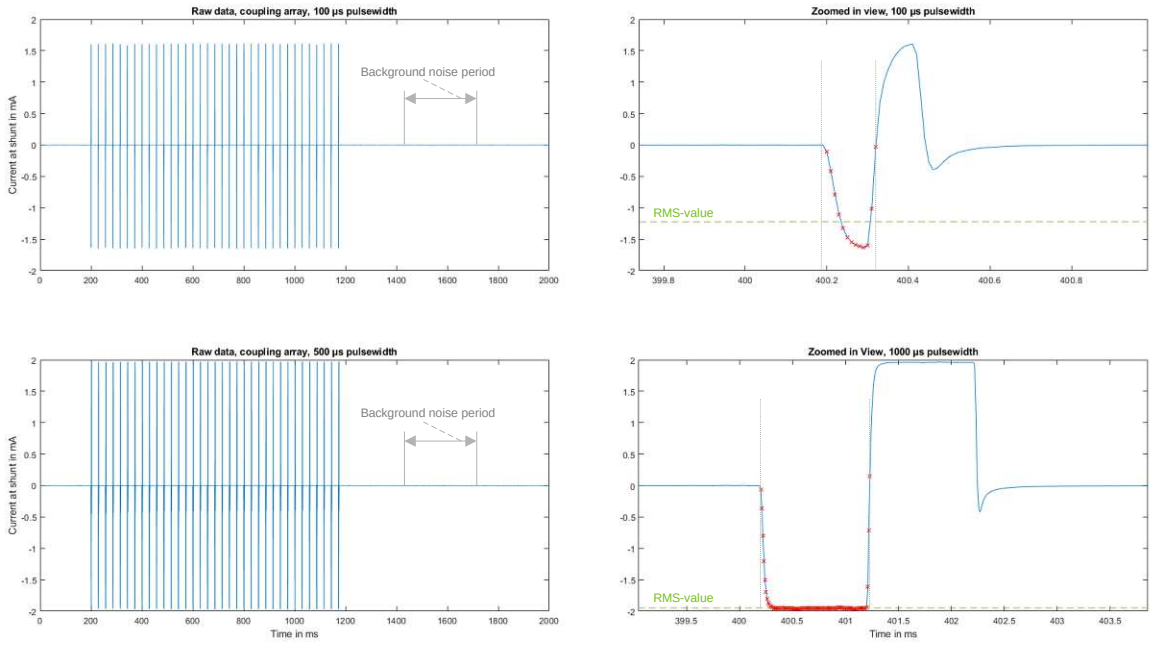

Figure 22: Raw data and peak shape of coupling array measurements. The top row shows the measurement data of a short pulse width (100 µs) and the bottom row shows a long pulse width (1000 µs). The right column is the zoomed in version of the left column, showing only a single peak to emphasize the difference in shape.

8.6.3 Analysis of cuff selectivity

"Selectivity" was defined as the percentage of maximal recruitment available at the primary muscle, before the secondary muscle starts to get active. The primary muscle was always the muscle with the lower threshold. Figure 23 shows the signal as it was measured by the EMG electrode. It measured the activation of the muscle. One of these CMAPs was received for each stimulation pulse on every channel measured. Each CMAP was described by its peak-to-peak voltage. Plotting these voltage values against the amplitude of the stimulation pulse produced recruitment curves (figure 24). The values in the curves in figure 24 were normalized to the highest level of activation achieved by the muscle during supra-maximal stimulation, i.e. at maximal stimulation amplitude. Values between two measurement points were determined through linear interpolation. These recruitment curves were used to determine the threshold currents for further evaluation. The threshold was set to 10% of the maximum activation of each muscles as this roughly corresponded with the activation of just noticeable contractions[21]. These threshold values are marked as vertical lines in figure 24.

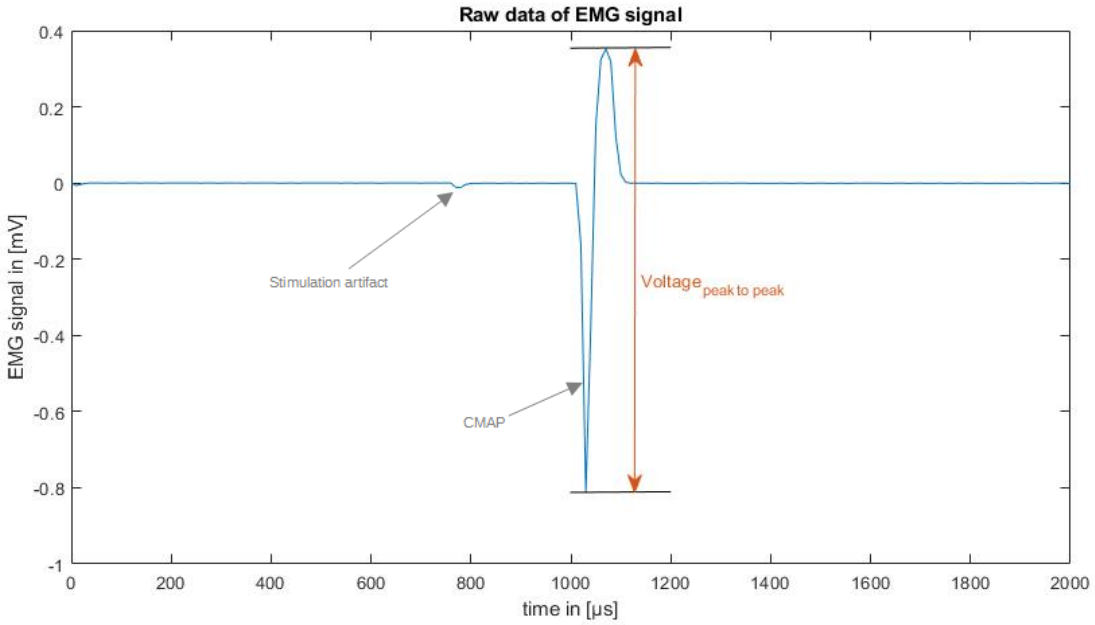

Figure 23: Raw signal measured by EMG electrode. For further evaluation the peak-to-peak voltage was used to represent the muscular response.

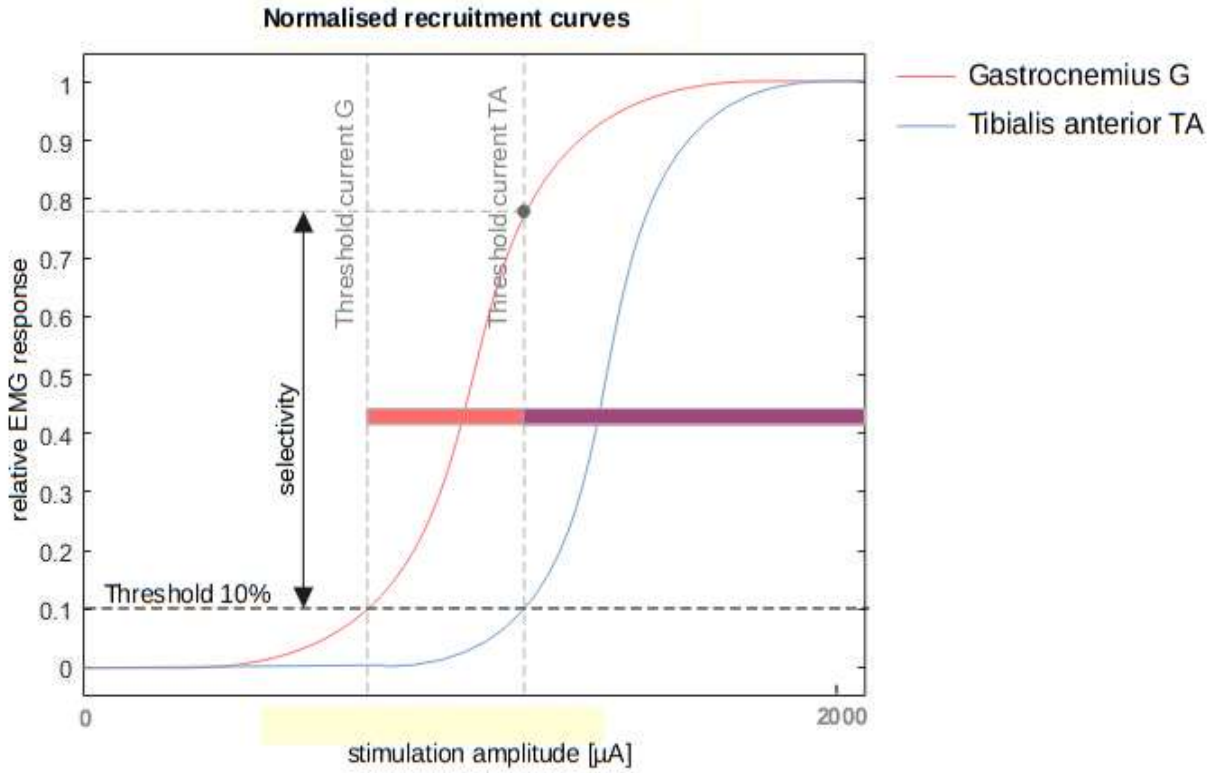

Figure 24: Recruitment curves for gastrocnemius and tibialis anterior muscles. Red lines show the reaction of the gastrocnemius muscle, blue lines show the reaction of the tibialis anterior muscle. The EMG values have been normalized in relation to the highest achieved activation of each muscle during the experiment.

The goal of the selectivity measurements was to determine, how well two muscles (i.e. tibialis anterior and gastrocnemius) could be controlled independently with a multi channel nerve cuff

electrode around the sciatic nerve. This was done by comparing the recruitment curves of both muscles and determining the percentage of maximal recruitment available at the primary muscle, before the secondary muscle starts to get active. Figure 24 also displays how the information in the recruitment curves can be displayed as a bar chart, showing which current ranges are necessary to activate the muscles. Red areas signify current ranges which activate only the gastrocnemius muscle, while blue areas show the ranges which activate only the tibialis anterior muscle. Purple areas represent activation of both muscles. Each channel of the multi channel nerve cuff electrode had its own recruitment curve and therefore different active current ranges for the two muscles. If both muscles had at least one channel which allowed for their selective activation before the other muscle started to counteract it, then selective stimulation was considered possible. Higher levels of selectivity correspond to a better performance of the cuff electrode. Figure 25 shows an example of such a bar graph representation for all 4 channels and the current ranges needed for selective activation.

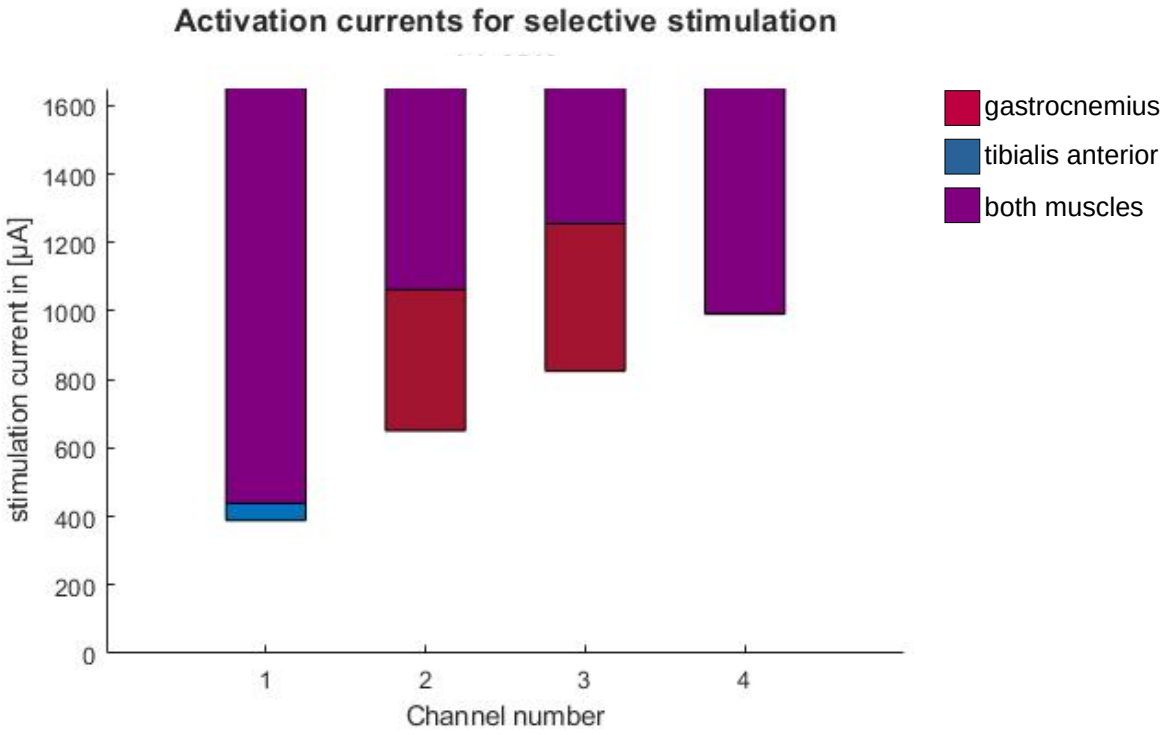

Figure 25: Current ranges allowing for selective stimulation of a single muscle. Red areas indicate a selective stimulation of the gastrocnemius muscle while blue areas show the selective stimulation of the tibialis anterior muscle. Purple areas activate both muscles and are therefore non-selective.

8.6.4 Analysis of the full system

As the cuff electrode was not supplied by a perfect array (with a crosstalk coefficient of 0%) stimulation occurred on more than one channel site. We developed two models to provide an estimate at which crosstalk coefficients selective activation of both muscles was possible. As the CorTec experiments provided the most data, these were used for the calculations in both models. The models were based on different assumptions:

Model 1

Assumptions:

- **The two stimulation sites are completely independent**
- **Crosstalk coefficients are symmetrical for both channels**

This means, that as long as the threshold for the single site is not reached no reaction occurs, no matter which sub-threshold current is applied to the second site.

Using the bar graphs representation we have determined the current ranges which were used for selective activation. However the electrode array in our system expressed a certain amount of crosstalk current to the secondary channels. This current induces stimulation on these channels, which had to be taken into account. Using the threshold values of the cuff electrode we determined the lowest crosstalk coefficient with which selective stimulation was still possible.

$$c_{high} = min\left(\frac{I_{thrG1}}{I_{thrTA2}}, \frac{I_{thrTA2}}{I_{thrG1}}\right)$$

Equation 7: higher crosstalk coefficient

In equations 7 and 8 the Index 1 refers to the channel preferring the gastrocnemius and the Index 2 refers to the channel preferring the tibialis anterior muscle. These numbers do not necessarily need to have the same numbering as the channels in the setup.

At crosstalk coefficients higher than c_{high} the crosstalk current on the secondary channel will induce stimulation before the stimulation threshold on the primary channel is reached. Therefore it wont be possible to activate both muscles separately. At crosstalk coefficients lower than c_{high} both muscles can be addressed separately by the implanted system (table 4).

In addition the maximum percentage of achievable activation was determined from the recruitment curves for the analysed channels. The strength of the muscle reaction was capped by the threshold of the secondary muscle on the same channel, while the allowed crosstalk coefficients were capped by the threshold of the secondary muscles on the secondary channels. This is captured by the following equation:

$$c_{low} = min\left(\frac{I_{thrTA1}}{I_{thrTA2}}, \frac{I_{thrG2}}{I_{thrG1}}\right)$$

Equation 8: lower crosstalk current ratio

At crosstalk coefficients lower than c_{low} the array stops to be the limiting factor. Instead the selectivity of the cuff electrode is the limiting factor for the system's performance. Reducing the crosstalk coefficient even further does not improve the performance of the joint system (table 4).

For full usability of the implant, only two channels were necessary, of which each favoured a different muscle. If more than one combination of 2 channels was possible for selective stimulation, the combination with the most forgiving crosstalk current ratios and the combination with the highest achievable muscle reaction was determined. Equations 7 and 8 were solved for both muscles leading to two different crosstalk current ratios. Since both muscles needed to be

selectively available, the stricter threshold (i.e. the smaller value) was the only relevant one. Therefore the higher value was discarded, as it did not hold any additional information.

Model 2

Assumptions:

- **Stimulation currents on multiple sites contribute lineary to achieving a joint stimulation threshold**.
- **Crosstalk coefficients are symmetrical for both channels.**

This means that achieving **x%** of threshold current on stimulation site 1 and achieving **(100-x)%** of threshold current on site 2 would result in threshold level activation of the muscle.

These joint thresholds were determined using the following conditions:

$$\frac{I_1}{I_{thrG1}} + \frac{I_2}{I_{thrG2}} \geq 1$$

Equation 9: Activation condition for the gastrocnemius

$$\frac{I_1}{I_{thrTA1}} + \frac{I_2}{I_{thrTA2}} \geq 1$$

Equation 10: Activation condition for the tibialis anterior

A value of 1 in those inequations corresponds to stimulation at threshold level. Higher values correspond to stronger levels of activation. I_1 and I_2 are the currents applied by channels 1 and 2 respectively. I_{thr} are the threshold values on these channels for the gastrocnemius (G) and tibialis anterior (TA) muscles.

Considering the crosstalk current, we formed the following conditions with the (still unknown) crosstalk coefficient c_{M2}:

for stimulation on site 1: $I_2 = c_{M2} \cdot I_1$

Equation 11

for stimulation on site 2: $I_1 = c_{M2} \cdot I_2$

Equation 12

These equations assume, that the crosstalk behaves symmetrical for both channels of the array.

Solving these equations numerically in MatLab (script in Appendix) provided the highest level of crosstalk which still allows for a minimal degree of selective control of each muscle separately (table 4). These threshold values describe the same state as the “higher crosstalk coefficient” benchmark in Model 1. Higher values result in the same muscle always activating before its counterpart. This model did not produce a threshold similar to the “lower crosstalk” benchmark. This means that according to this model a reduction in crosstalk current ratio will always result in an improved system performance.

The performance of the system was described by determining its selectivity analogously to the performance of the nerve cuff electrode alone.

Table 4 gives an overview of the effects of the crosstalk coefficient on the relationship between the selectivity of the full system and the crosstalk coefficient of the coupling array.

Model 1	
crosstalk coefficient	**properties**
c > c_high	no selective stimulation of both muscles possible
c_high > c > c_low	selective stimulation is possible. Coupling array and cuff electrode both influence the selectivity of the full system.
c_low > c	selective stimulation possible. Lowering the crosstalk coefficient even further does not improve the selectivity of the full system.
Model 2	
crosstalk coefficient	**properties**
c > c_M2	no selective stimulation of both muscles possible
c_M2 > c	selective stimulation is possible. Coupling array and cuff electrode both influence the selectivity of the full system.

Table 4: The effect of the crosstalk coefficient on the properties of the full system according to Model 1 and Model 2

9 Results

9.1 Preliminary measurements

During the preliminary measurements the area of the electrodes proved to be too small to achieve current transfer through capacitive coupling, thus the electrodes in the final design were not insulated.[17] The experiments also showed, that electrode gel was necessary for sufficient current to be transferred through the skin. The short bursts, that should have been transferred capacitively were not suitable for further evaluation as they were not even remotely of rectangular shape. The setup was reliant on the flow of current over the resistive path. Figure 26 shows the difference in signal shape transmitted by an array with electrode gel and the same array without gel. It clearly shows, that the resistance was much too big, to transfer the rectangular signal. Only the edges of the signal can be distinguished as a short peak.

The preliminary measurements also showed, that the first design of the electrode array, which consisted of four electrodes was too large and failed under the mechanical stress during *in vivo* conditions. To reduce mechanical stress on the implant as well as to improve animal welfare, we changed the design of the implant, reducing its size from four to two channels.

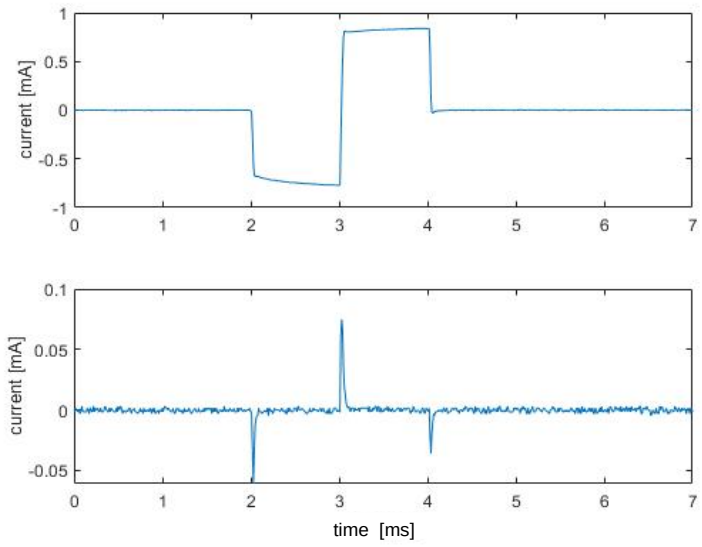

Figure 26: A comparison of the transmitted current via the electrode array with electrode gel (top) and without electrode gel (bottom)

9.2 Survival of test subjects

The surgery proved to be very demanding on the animals so that not all experiments could be carried out as intended by the original measurement plan. The following table shows the number of days the test subjects survived after the implantation procedure. The planned duration of the experiment was 12 weeks (84 days) after surgery. Only 1 of the 10 animal subjects survived the entire experiment. 3 animals died shortly after the implantation procedure. The mean value for the number of days survived was 33.1 with a standard deviation of 23.5. This value does not take the

animals into account, that died on the day of surgery. This data can be seen in table 5. A full timeline of measurements that were performed is provided in the appendix (table I).

Survival

Animal	Surgery	Death	Days
A1	08.04.21	08.04.21	0
A2	08.04.21	08.04.21	0
A3	15.04.21	14.05.21	29
A4	15.04.21	05.07.21	81
A5	29.04.21	07.06.21	39
A6	29.04.21	19.05.21	20
A7	05.05.21	10.06.21	36
A8	05.05.21	05.05.21	0
A9	20.05.21	07.06.21	18
A10	20.05.21	29.05.21	9
		Mean	33.1
		SD	23.5

Table 5: Survival length of animal subjects after surgery, animals that died the same day (A1, A2 and A8) were excluded for the calculation of the mean number of survival days.

9.3 Implant lifetime and component failure

The impedance measurements were performed to determine the life expectancy of the implant under *in vivo* conditions. The amount of mechanical stress due to the rats movement caused wires to break. The exact timing of the wire failure could not be determined, as measurements were not carried out daily. However the following table shows the number of days, at which the first wire breakage was detected during a measurement. Subjects which died before any wire broke are marked as “x” and not taken into account for the mean value of 24 days (SD = 11 days). This data can be seen in table 6. Single broken wires did not disqualify the animal from all measurements. If certain measurements were still possible to perform, these were carried out according to the measurement protocol.

First component failure

Animal	Surgery	First failure	Days	Type of failure
A1	08.04.21	-	x	death of subject
A2	08.04.21	-	x	death of subject
A3	15.04.21	14.05.21	29	internal array CH1 not responding
A4	15.04.21	27.05.21	42	internal array CH1 not responding, weak magnetic contact
A5	29.04.21	27.05.21	28	Cuff GND broken, Cuff CH2 and CH2 not very responsive
A6	29.04.21	19.05.21	20	Cuff CH3 not responding
A7	05.05.21	19.05.21	14	internal array CH1 not reponding, cuff CH4 not responding
A8	05.05.21	-	x	death of subject
A9	20.05.21	02.06.21	13	no strong (magnetic) contact of the external array possible
A10	20.05.21	-	x	death of subject
		Mean	24.3	
		SD	11.0	

Table 6: Time before first wire breakage was detected

9.4 Coupling properties of the array, crosstalk coefficient

Table 7 shows the current distribution between the channels during the array measurements. Fig. 27 shows a graphical representation of this data. Faulty measurements due to broken wires are marked in red. During these measurements the entire current flowed through the remaining unbroken channel. In measurements *"A7_0519"* and *"A7_0602"* the implanted array was twisted, and only one of the channels could be aligned well. The names of the experiments include the subject name and the date of the measurement in the following format: "*Name_MMDD*". This nomenclature is consistent for all measurements performed.

Arraytests

Experiment	Input Ch1				Input Ch2			
	Receive Ch1		Receive Ch2		Receive Ch1		Receive Ch2	
	Mean	SD	Mean	SD	Mean	SD	Mean	SD
	%	%	%	%	%	%	%	%
A3_0428	50.14	0.07	49.86	0.06	53.44	0.04	46.56	0.03
A4_0428	50.52	0.07	49.48	0.06	52.57	0.07	47.43	0.06
A4_0527	0.85	0.00	99.15	0.03	0.58	0.00	99.42	0.05
A5_0512	51.71	0.05	48.29	0.04	49.23	0.07	50.77	0.07
A5_0527	51.11	0.07	48.89	0.07	48.29	0.07	51.71	0.07
A6_0512	51.87	0.06	48.13	0.06	50.76	0.03	49.24	0.28
A6_0519	53.33	0.07	46.67	0.06	51.22	0.07	48.78	0.06
A7_0519	99.71	0.13	0.29	0.00	99.65	0.13	0.35	0.00
A7_0602	3.72	0.00	96.28	0.10	3.54	0.00	96.46	0.08
A9_0602	49.04	0.06	50.96	0.06	42.13	0.06	57.87	0.07
Mean	51.10	0.06	48.90	0.06	49.66	0.06	50.34	0.09
SD	1.38	0.01	1.38	0.01	3.77	0.02	3.77	0.08

Table 7: Current distribution of array measurement. The intended current path is to be received on the same channel as the input is given (i.e. if the input is on Ch1, then Ch1 is the intended recipient). This is the "primary channel". Mean and SD values do not take excluded (marked red) into account. These measurements were excluded because not all channels were properly connected or an internal wire was broken.

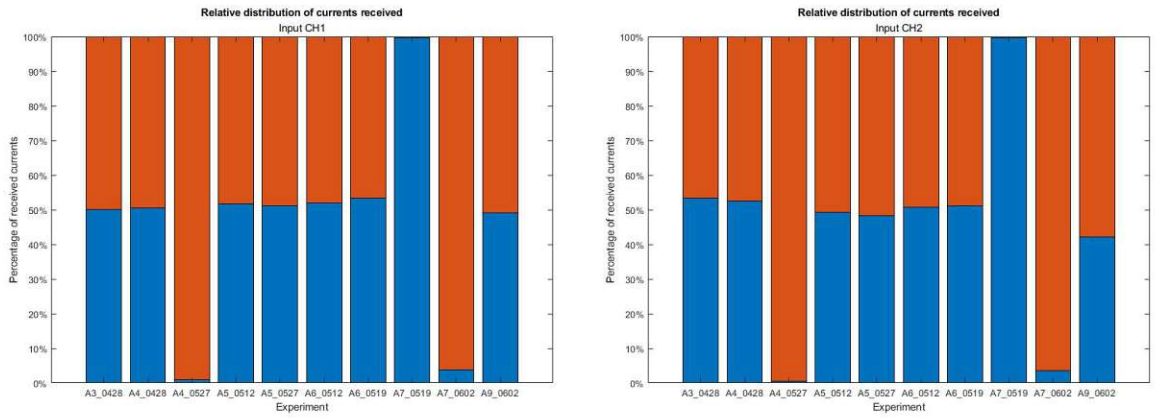

Figure 27: Current distribution during array measurements. Measurements where all the current is received on one channel were caused by broken wiring or twisting of the implant. They were not considered in further evaluation.

Figure 28 shows the percentage of current following the intended current path after excluding the faulty measurements marked in red (table 7). The average value obtained over all experiments is 50.6% with a standard deviation of 2.8%. For test subjects with more than one measurement

available, the development over time is shown as well. Array measurements were not performed on the day of surgery (i.e. day 0), and the first measurement was always on day 13.

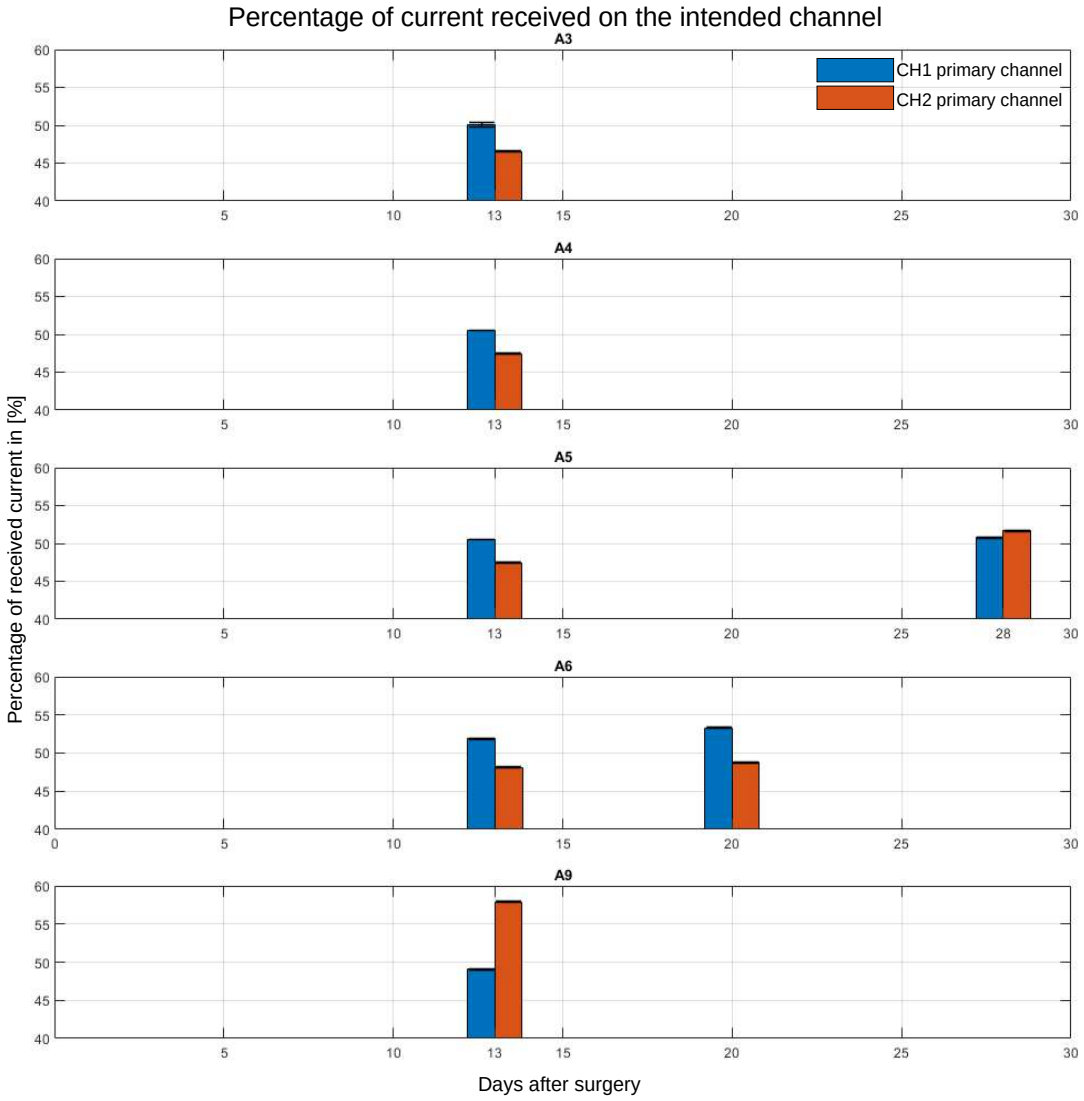

Figure 28: Percentage of the received current on the primary channel, excluding faulty measurements. For test subjects where more than one measurement was successfully performed, the development over time can be seen.

Table 8 shows the crosstalk coefficients determined during the measurements of the array. Values above 100% mean, that more current is flowing on the secondary channel than on the primary channel. An ideal array has a crosstalk coefficient of 0%.

Crosstalk coefficient

Experiment	Input Ch1	Input Ch2
A3_0428	99 %	115 %
A4_0428	98 %	111 %
A5_0512	93 %	97 %
A5_0527	96 %	93 %
A6_0512	93 %	103 %
A6_0519	88 %	105 %
A9_0602	104 %	73 %

Table 8: The crosstalk coefficients describe the amount of current received on the secondary channel in relation to the primary channel. Lower values correspond to better array performance.

9.5 Selectivity Measurements

The selectivity was defined as the percentage of maximal recruitment available at the primary muscle, before the secondary muscle starts to get active.

9.5.1 Selectivity of the cuff electrode, CorTec setup

The selectivity of the nerve cuff electrode was determined using pulses of increasing phase width and amplitude by comparing the recruitment curves of the muscles. Table 9 shows the selectivity for the lowest phase width producing distinguishable reactions of the muscles. In most cases, this was the lowest used phase width of 10 µs. The phase width which was used is provided in table 9. Channels on which the gastrocnemius muscle responded first have the selectivity marked as red, while channels on which the tibialis anterior muscle responded first have been marked in blue.

Thresholds and selectivity Cortec

	Cuff – Ch1			Cuff – Ch2			Cuff – Ch3			Cuff – Ch4			
Experiment	Th_gastro	Th_tibialis	Selectivity	Th_gastro	Th_tibialis	Selectivity	Th_gastro	Th_tibialis	Selectivity	Th_gastro	Th_tibialis	Selectivity	Phase width
	µA	µA	%	µA	µA	%	µA	µA	%	µA	µA	%	µs
A3_0428	953	1043	25	1114	1154	4	971	1008	0	758	773	4	**10**
A4_0415	439	388	54	650	1062	85	824	1266	89	991	991	0	**10**
A4_0428	1109	1383	55	192	196	0	187	194	0	1451	1282	17	**10**
A4_0519	439	388	54	650	1062	85	824	1255	89	991	992	0	**10**
A4_0527	835	804	21	816	949	28	859	914	21	962	817	53	**10**
A4_0610	985	1005	0	920	1250	50	866	924	22	720	763	0	**10**
A4_0705	923	972	14	914	967	18	149	158	0	197	233	0	**10**
A5_0429	1166	1183	0	1615	1550	0	1606	908	19	1700	1676	0	**10**
A5_0512	244	175	74	58	42	0	204	243	40	230	266	53	**100**
A5_0527	N/A	N/A	N/A	N/A	N/A	N/A	1307	1167	8	612	779	49	**100**
A6_0429	987	805	42	1091	932	27	1070	885	26	869	671	30	**10**
A6_0512	847	828	0	780	758	14	916	921	0	977	1075	41	**10**
A6_0519	966	782	63	1178	972	34	N/A	N/A	N/A	1212	1073	24	**10**
A7_0505	10	13	0	535	512	14	498	467	20	336	298	33	**100**
A7_0519	7	9	0	1134	1209	27	1211	1250	15	6	4	0	**10**
A7_0602	N/A	N/A	N/A	N/A	N/A	N/A	1380	1226	61	N/A	N/A	N/A	**10**
A7_0610	N/A	N/A	N/A	N/A	N/A	N/A	N/A	N/A	N/A	N/A	N/A	N/A	**10**
A8_0505	295	226	55	309	256	41	348	268	57	337	263	49	**100**
A9_0520	725	1103	64	9	7	0	N/A	N/A	N/A	N/A	N/A	N/A	**10**
A9_0602	887	859	12	7	1	0	7	1	0	10	17	0	**10**
A10_0520	1045	930	32	930	1045	0	1268	1168	20	19	11	0	**10**

Gastrocnemius responds before Tibialis Anterior
Tibialis Anterior responds before Gastrocnemius
No selectivity ; both muscles have the same threshold

Table 9: Selectivity of the nerve cuff, CorTec setup. The table shows the stimulation channel for both muscles on each channel as well as the achievable selectivity. The data refers to the lowest phase width at which selective behaviour was observed. If no selective behaviour was observed the selectivity is marked in yellow as 0%. Measurements marked in grey as "N/A" did not produce recruitment curves due to mechanical failure and could therefore not be evaluated.

Out of a total of 18 measurements on 7 animals a total of 7 measurements on 3 different animals allowed for selective control of both muscles. Measurements in which not all recruitment curves could be determined due to broken wires were excluded, with the exception of "A5_0527", as the 2 working channels each activated a different muscle, thus still fulfilling the requirement of at least one channel being able to activate each muscle separately. All measurements allowed for the selective control of at least one muscle.

Figure 29 displays an example of the bar graph representation of the stimulation currents for selective stimulation using the CorTec setup. The test subject A4 was chosen to show the development over time, as this was the only animal which survived for the intended duration of the experiments. Red areas in the bars show the current ranges that only stimulate the gastrocnemius muscle and blue areas stimulate the tibialis anterior muscle. Purple areas activate both bars and were therefore not selective. The maximum selectivity which could be achieved during each

experiment is also provided accordingly. The bar graphs for all remaining CorTec experiments can be found in the appendix in figures I - IV.

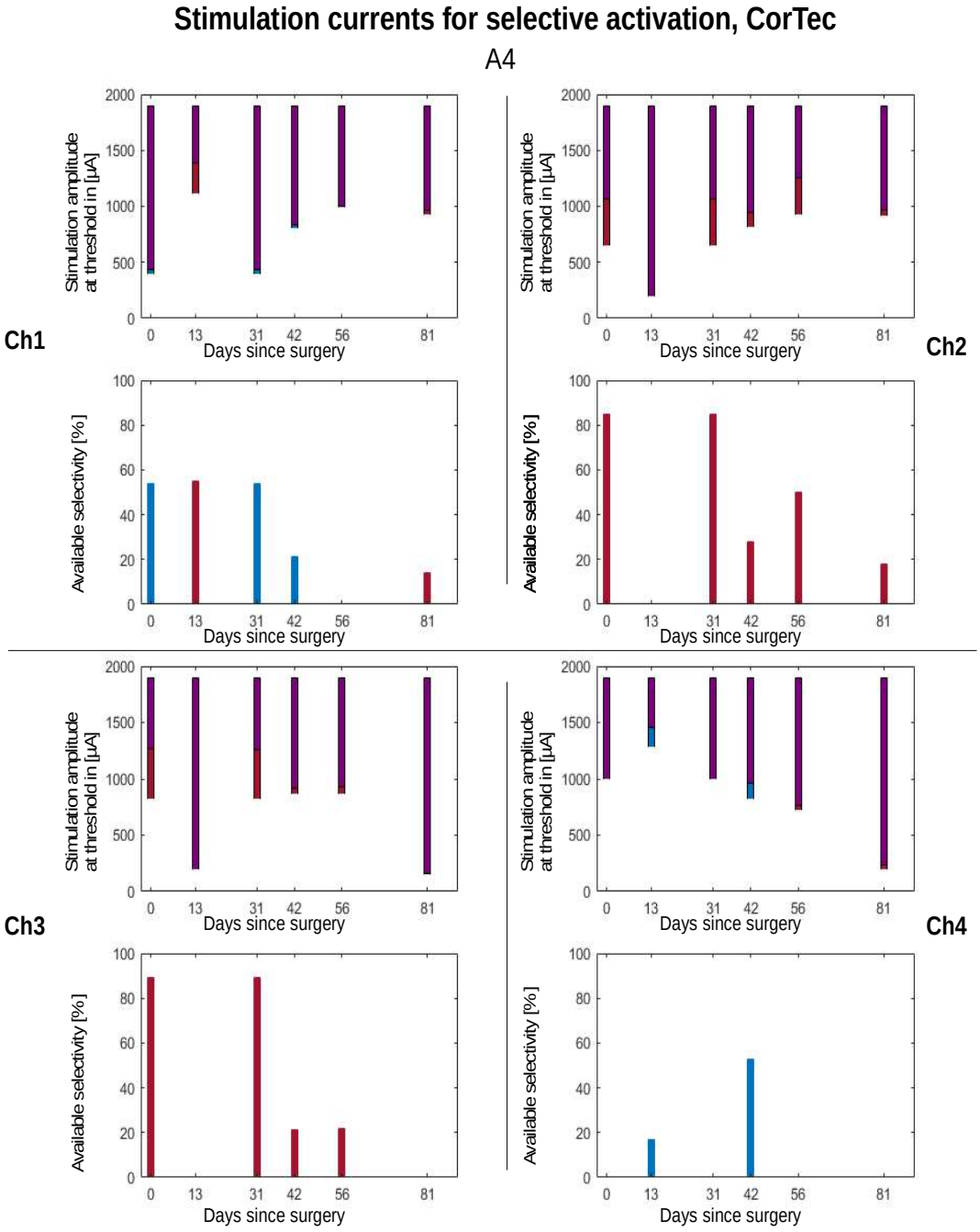

Figure 29: Development of activation currents for selective stimulation over time after surgery for test subject A4. Red areas show currents which stimulate only the gastrocnemius muscle while blue areas show currents which only stimulate the tibialis anterior muscle. Purple areas activate both muscles. In addition the maximum achievable selectivity during each experiment is provided for gastrocnemius (red) and tibialis anterior (blue). CorTec setup

9.5.2 *Selectivity of the nerve cuff electrode using the Isis setup*

The selectivity of the nerve cuff electrode was determined using pulses of increasing phase width and comparing the recruitment curves of the muscles. Table 10 shows the selectivity for the lowest phase width producing distinguishable reactions of the muscles. In most cases, this was the lowest used phase width of 50 µs. The phase width which was used is provided in table 10. The first two channels (1+2) and the last two (3+4) channels were connected in this setup, effectively converting the 4-channel nerve cuff electrode into a 2-channel electrode. Channels on which the gastrocnemius muscle responded first have the selectivity marked as red while channels on which the tibialis anterior muscle responded first have been marked in blue.

Thresholds and selectivity ISIS

Experiment	Ch1+2			Ch3+4			
	Th_gastro	Th_tibialis	Selectivity	Th_gastro	Th_tibialis	Selectivity	Phase width
	µA	µA	%	µA	µA	%	µs
A3_0428	254	203	31	215	154	33	**50**
A4_0428	271	306	16	302	254	13	**50**
A4_0519	204	171	27	263	215	43	**50**
A4_0527	170	178	0	200	164	29	**50**
A4_0610	138	155	21	200	203	0	**50**
A4_0705	305	305	0	258	164	85	**50**
A5_0512	355	305	29	325	401	62	**50**
A5_0527	N/A	N/A	N/A	N/A	N/A	N/A	**50**
A6_0512	166	167	0	250	250	0	**50**
A6_0519	418	359	65	502	425	62	**50**
A7_0519*	178	209	27	157	111	47	**100**
A7_0602	1405	1405	0	360	304	59	**50**
A7_0610	N/A	N/A	N/A	304	266	21	**50**
A9_0602	N/A	N/A	N/A	N/A	N/A	N/A	**50**

Gastrocnemius responds before Tibialis Anterior
Tibialis Anterior responds before Gastrocnemius
No selectivity ; both muscles have the same threshold

Table 10: Selectivity of the nerve cuff, Isis setup. The table shows the stimulation channel for both muscles on each channel as well as the achievable selectivity. The data refers to the lowest phase width at which selective behaviour was observed. If no selective behaviour was observed the selectivity is marked in yellow as 0%. Measurements marked in grey as "N/A" did not produce recruitment curves due to mechanical failure and could therefore not be evaluated.

Out of a total of 11 measurements on 5 animals a total of 3 measurements on 3 different animals allowed for selective control of both muscles. Measurements in which not all recruitment curves could be determined due to broken wires were excluded. Out of these 11 measurements selective control of one muscle was possible in 10 cases.

Figure 30 displays an example of the bar graph representation of the stimulation currents for selective stimulation using the Isis setup. The test subject A4 was chosen to show the development over time, as this was the only animal which survived for the intended duration of the experiments. Red areas in the bars show the current ranges that only stimulate the gastrocnemius muscle and blue areas stimulate the tibialis anterior muscle. Purple areas activate both bars and are therefore non

selective. The maximum selectivity which could be achieved during each experiment is also provided accordingly.

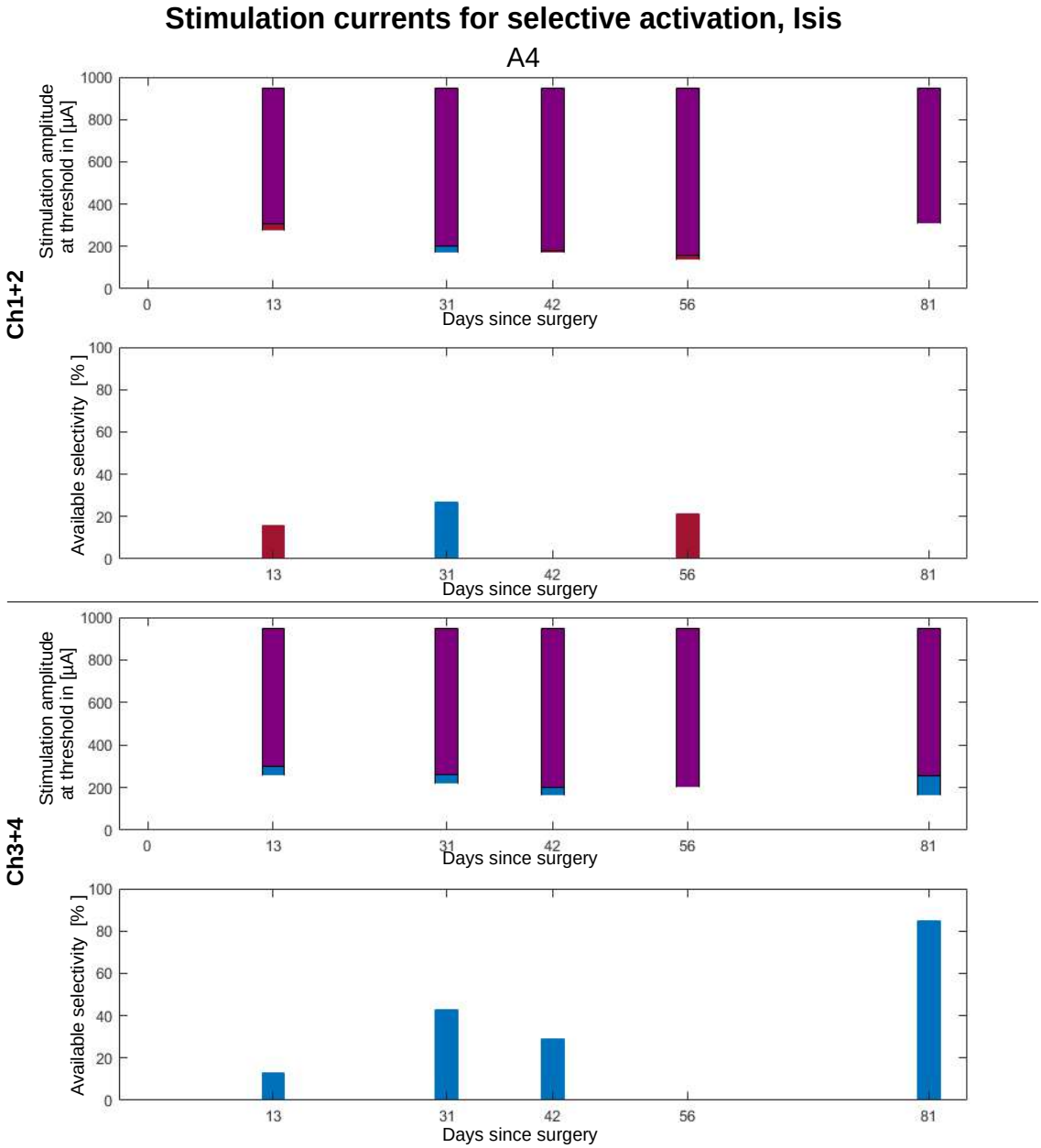

Figure 30: Development of activation currents for selective stimulation over time after surgery for test subject A4. Red areas show currents which stimulate only the gastrocnemius muscle while blue areas show currents which only stimulate the tibialis anterior muscle. Purple areas activate both muscles. In addition the maximum achievable selectivity during each experiment is provided for gastrocnemius (red) and tibialis anterior (blue). Isis setup

The bar graph representation of the remaining experiments can be found in the appendix in figures V and VI.

Selectivity of nerve cuff electrode + surface ground, Isis setup

The selectivity of the nerve cuff electrode was determined using pulses of increasing phase width and comparing the recruitment curves of the muscles. Table 11 shows the selectivity for the lowest phase width producing distinguishable reactions of the muscles. In most cases, this was the lowest used phase width of 50 µs. The first two channels (1+2) and the last two (3+4) channels were connected in this setup, effectively converting the 4-channel nerve cuff electrode into a 2-channel electrode. Channels on which the gastrocnemius muscle responds first have the selectivity marked as red while channels on which the tibialis anterior muscle responds first have been marked in blue.

Threshold and Selectivity ISIS+SG

	Ch1+2			Ch3+4			Phase width
Experiment	**Th_gastro**	**Th_tibialis**	**Selectivity**	**Th_gastro**	**Th_tibialis**	**Selectivity**	**µs**
	µA	**µA**	**%**	**µA**	**µA**	**%**	
A3_0428	116	112	0	105	57	19	**100**
A4_0428	133	113	0	139	203	15	**50**
A4_0519	102	49	21	100	36	28	**50**
A4_0527	102	42	15	12	23	0	**100**
A4_0610	123	111	0	102	106	0	**50**
A4_0705	142	145	0	226	142	39	**50**
A5_0512	11	11	0	227	312	40	**50**
A5_0527	378	442	23	282	413	43	**50**
A6_0512	146	129	0	145	143	0	**50**
A6_0519	105	35	31	101	27	38	**50**
A7_0519	113	112	0	107	43	28	**100**
A7_0602	N/A	N/A	N/A	N/A	N/A	N/A	**50**
A7_0610	N/A	N/A	N/A	N/A	N/A	N/A	**50**
A9_0602	714	562	71	546	439	55	**50**

Gastrocnemius responds before Tibialis Anterior
Tibialis Anterior responds before Gastrocnemius
No selectivity ; both muscles have the same threshold

Table 11: Selectivity of nerve cuff and surface ground, Isis setup with surface ground electrode. The table shows the stimulation channel for both muscles on each channel as well as the achievable selectivity. The data refers to the lowest phase width at which selective behaviour was observed. If no selective behaviour was observed the selectivity is marked in yellow as 0%. Measurements marked in grey as "N/A" did not produce recruitment curves due to mechanical failure and could therefore not be evaluated.

Out of a total of 12 measurements on 9 animals none of the experiments allowed for selective control of both muscles. Measurements in which not all recruitment curves could be determined due to broken wires were excluded. Out of these 12 measurements, selective control of a single muscle was possible in 10 measurements on 9 different animals.

The bar graph representation of these experiments can be found in the appendix in figures VII - VIII.

9.5.3 Selectivity of the entire system, Isis setup

Due to different mechanical failures throughout the system, not all recruitment curves could be measured. Several experiments did not produce recruitment curves on any channel and are therefore not included in the table. This was the case for the following experiments:

"*A4_0527*", "*A4_0610*", "*A5_0527*", "*A7_0519*", "*A7_0602*", "*A9_0602*"

If only one channel did not produce results, the respective cells have been marked in grey as "N/A" in table 12. The full system did not show selective behaviour in any of the experiments. All measurements were performed with a pulse width of 50 µs.

Threshold and Selectivity Fullsystem

Experiment	Ch1+2			Ch3+4			
	Th_gastro	Th_tibialis	Selectivity	Th_gastro	Th_tibialis	Selectivity	Phase width
	µA	µA	%	µA	µA	%	µs
A3_0428	2067	1708	48	2157	1907	42	**50**
A4_0428	1573	1389	12	1731	1688	11	**50**
A5_0512	2122	2221	25	2029	2251	41	**50**
A5_0527	N/A	N/A	N/A	3355	3413	13	**50**
A6_0512	2065	1961	22	N/A	N/A	N/A	**50**
A6_0519	1928	1746	44	1900	1710	30	**50**
A7_0610	73	110	14	N/A	N/A	N/A	**50**

Table 12: Selectivity of the full system (Isis setup with transfer array and surface ground electrode). The table shows the stimulation channel for both muscles on each channel as well as the achievable selectivity. Measurements marked in grey as "N/A" did not produce recruitment curves due to mechanical failure and could therefore not be evaluated.

Out of a total of 4 measurements on 4 animals none of the experiments allowed for selective control of both muscles. Measurements in which not all recruitment curves could be determined due to broken wires were excluded. Selective control of a single muscle was possible in all measurements.

9.5.4 Evaluation using model 1 and model 2

The crosstalk threshold in table 13 describes the maximum percentage of current allowed on the secondary channel relative to the primary channel. The higher level corresponds to stimulation at threshold level (i.e. 10% of maximal recruitment) of the primary muscle on the secondary channel (which is the antagonist of the primary muscle on the primary channel), the lower level corresponds to the threshold of the secondary muscle on the primary channel. The values in table 13 have been determined using model 1 for the channel pairs which allowed for the most forgiving crosstalk coefficients. Similarly in table 14 the crosstalk benchmarks have been determined with model 1 for producing the highest possible muscle activation. Applying model 2 we receive the values in table 15.

Crosstalk benchmarks, most forgiving, Model 1, CorTec

	higher crosstalk	lower crosstalk	max activation G	max activation TA
A4_0428	87 %	76 %	55 %	17 %
A4_0519	60 %	37 %	85 %	54 %
A4_0527	95 %	89 %	21 %	53 %
A5_0512	86 %	72 %	40 %	74 %
A5_0527	52 %	47 %	49 %	8 %
A6_0512	78 %	70 %	41 %	14 %

Table 13: Limiting crosstalk benchmarks of the system. Values are chosen for the channel pairs with the most forgiving crosstalk current ratios. G = gastrocnemius, TA = tibialis anterior, Model 1, CorTec setup

Crosstalk benchmarks, strongest activation, Model 1, CorTec

	higher crosstalk	lower crosstalk	max activation G	max activation TA
A4_0428	87 %	76 %	55 %	17 %
A4_0519	47 %	31 %	89 %	54 %
A4_0527	100 %	85 %	28 %	53 %
A5_0512	76 %	66 %	53 %	74 %
A5_0527	52 %	47 %	49 %	8 %
A6_0512	78 %	70 %	41 %	14 %

Table 14: Limiting crosstalk benchmarks of the system. Values are chosen for the channel pairs with the highest possible muscle activation. G = gastrocnemius, TA = tibialis anterior, Model 1, CorTec setup

Crosstalk benchmark, Model 2, CorTec

experiment	max crosstalk
A4_0428	47 %
A4_0519	47 %
A4_0527	33 %
A5_0512	43 %
A5_0527	23 %
A6_0512	31 %

Table 15: Limiting crosstalk benchmarks of the system. Model 2, CorTec setup

10 Discussion

10.1 Survival of test subjects and implant lifetime

Based on the acquired data, the implant in its current form seemed to be too invasive to be tolerated by the rat model. Adaptations need to be made in order to perform studies over an extended period of time. The size of the implant in comparison to the rat was relatively large, causing strain on both mechanical components and animal. As a result, neither the implants nor the rats survived for the entire experiment duration, which was intended to be 12 weeks. One test subject survived for almost the intended duration (81 of 84 days). Nevertheless wire breakage was detected on average 24 days after implantation. The head stage component proved to be very demanding on the animal as the skin around it did not heal properly. The fixation with a screw and bone cement proved to be not strong enough to be reliable and the head stage came loose in several test subjects.

The size of the array component of the implant was already drastically reduced after the preliminary measurements but still ended up being too large for the animal. Similar implants have been studied in dogs by Peckham et al.[22]. These implants had no percutaneous elements as they used inductive coupling and were much smaller compared to the size of the test subject. Peckham et al. report implant lifetimes of over 540 days in two cases and 180 days in one case. This supports the thesis, that a reduction in size in relation to the animal as well as the removal of percutaneous elements would greatly improve the animal and implant lifetimes.

Due to the unexpectedly short lifespan of most test subjects as well as the mechanical failures in the equipment, not all experiments could be performed as planned in the original timetable.

10.2 Coupling properties of the array

The measurements of the coupling properties of the array showed, that the transferred current was split almost equally on the two receiving channels. The measurements showed, that the values were not constant over time in a test subjects. As the internal array slightly shifted its position with the movement of the *in vivo* surrounding, the alignment of the electrodes changed slightly and impacted the distribution of current and therefore the selectivity. In the most extreme cases, the entire array ended up twisted and folded, making the correct contacting of both electrodes rather difficult.

The array was not selective in its current state, and a direct stimulation without implanted electronic components was not possible using the current design. A collagen capsule filled with conductive fluid formed around the transfer array, leading to a short circuit between the two channels of the implanted array. This is an issue that arose only under *in vivo* conditions and needs to be considered in further implant development. Krenn et al.[23] performed experiments on similar electrode arrays, which had square electrodes (9 mm x 9 mm) with an edge-to-edge pitch of 6 mm. They found that if the electrode share the same layer of hydrogel, the crosstalk coefficient was 80%[23], but if the electrodes were coated in separate strips of hydrogel, the crosstalk coefficient reached 22%. Therefore it can be expected, that the crosstalk coefficient of the implant will greatly improve, if the channels of the internal array are insulated from one another. This should be considered for further development of the array. Slight shifts in the alignment of the implant evoked relatively large

changes in the current distribution. However, it can be considered that the alignment by magnet is sufficiently consistent after the healing process has finished. The effects of the healing process could not be analysed thoroughly, as not enough measurements could be performed in the later stages of the experiment. Unfortunately the only test subject surviving for the intended duration suffered from wire breakage and the last successful array measurement was performed only 13 days after the surgery. Only two test subjects allowed for more than one successful array measurement. Of these, one showed unchanged current distribution between days 13 and 20 after implantation while the other one showed a noticeable change in current distribution between days 13 and 28 as the performance on channel 2 improved, which can be seen in figure 28. These measurements do not bear any statistical significance, however they suggest, that it might not be enough to determine the performance of the array shortly after surgery, but it might be necessary to wait for the healing process to conclude. No statement can be made at this point, whether the performance of the transfer array will be consistent after the healing process is concluded. We expected the animals to have sufficiently healed after 2 weeks, as the Veterinary Guidelines for Rodent Survival Surgery[24] by The Ohio State University suggest that the animal is ready to have its sutures and wound clips removed after 10-14 days. However certain areas, such as the tissue around the head stage socket protruding the skin did not heal properly at all and were in a constant state of inflammation. Therefore the duration of the healing period still needs to be assessed once the implants design has been adapted to be better received by the rat model.

10.3 Selectivity of the cuff electrode

10.3.1 CorTec setup

The CorTec experiments produced similar results as Tarler et al.[25] who found that in 64% of cases (23 / 36) an electrode would selectively activate a muscle in an *ex vivo* environment. Stimulation with the CorTec stimulator achieved this in 74% of cases (68 / 92). Tarler et al. used steering currents to raise the amount to 33 out of 36 cases[25], totalling to 92% of cases. They report that even though almost every electrode stimulated one muscle selectively, it was not always possible to achieve selective activation of all muscles in the same subject[25]. This is also true for our experiments, as we could achieve selective activation of both muscles only in 7 out of 18 experiments (39%) on 3 out of 7 animals (43%). Veraart et al.[26] was able to achieve selective activation in 6 out of 6 experiments for the medial gastrocnemius and the tibialis anterior with the lowest selectivity at 63% using steering currents. Although the experiments by Tarler et al.[25] and Veraart et al.[26] were performed on a different animal model (cats) and under *ex vivo* conditions, their success in implementing steering currents should be strongly considered when further developing the implant. The development over time was also evaluated for animal "*A4*" as this was the longest living subject (figure 29). The stimulation thresholds changed over time, however they did not follow a clearly distinguishable pattern. The development over time needs to be determined in further experiments once the mortality of test subjects in the experiments has been reduced. It would be of particular interest, if the stimulation thresholds stop changing at some point in time.

10.3.2 Isis setup

The experiments using the Isis setup and the internal ground electrode of the cuff produced similar results to the CorTec experiments, as selective activation of a muscle was achieved in 74% of cases (17 / 23). Selective activation of both muscles was possible in 3 out of 11 measurements (27%) on 3 out of 5 animals (60%). The percentage of measurements which allowed for selective stimulation is lower compared to the CorTec experiments. This is partly due to the higher phase width at which the Isis stimulator operated, which reduced the threshold difference between fascicles[18]. The lowest phase width of the Isis stimulator was 50 µs while for the CorTec stimulator was 10 µs. Due to the larger phase width, the necessary stimulation amplitudes were lower using the Isis stimulator. Just as in the CorTec experiments only animal "*A4*" provided data for the evaluation of the development over time. No distinguishable pattern could be found. Figure 30 shows the development of the stimulation thresholds and the achievable selectivity over the course of the experiments for test subject "*A4*".

10.3.3 Isis setup + surface ground

Upon replacing the internal cuff-ground electrode with a surface electrode placed on the animals skin, selective stimulation of the muscles could no longer be achieved. We suspect that this is due to the more diffuse electrical field and the weaker localization of charge in the nerve, however due to the limited amount of measurements and data, the influence of the surface ground electrode could not be further specified. Even though no selective control of both muscles was possible, in 10 out of 12 measurements the selective control of a single muscle was achieved.

10.4 Full system

Stimulation with the entire system was not selective, as every component in the system needs to perform sufficiently well to achieve selectivity as a whole. However we did manage to transfer enough current through the skin using the coupling array to evoke selective activation of a single muscle in 4 out of 4 cases.

10.4.1 Evaluation using Model 1 and Model 2

Model 1

The thresholds in tables 13 - 15 were used to determine rough benchmarks for the crosstalk coefficient needed from a coupling array to still allow for selective stimulation of the full system. The results in tables 13 and 14 assumed, that there is no interaction between two separate stimulation sites on the nerve (model 1). The higher crosstalk benchmark (table 13), is the most optimistic threshold. At crosstalk coefficients above this benchmark no selectivity can be achieved, as the current on the secondary channel will induce stimulation before the stimulation threshold on the primary channel is reached. The selectivity which was possible with the nerve cuff electrode by itself can not be achieved due to the stimulation on the secondary channel. The lower crosstalk benchmark (table 14) gives the value at which the electrode cuff becomes the limiting factor for the selectivity of the system. Under these conditions a further improvement of the coupling array does not improve the selectivity of the full system. This is because the counteracting muscle is activated on the same channel of the nerve cuff electrode as the primary muscle. Therefore a further focusing

of the current onto the same channel by the coupling array no longer changes the selectivity of the full system. For crosstalk coefficients between the higher and lower crosstalk benchmark the selectivity of the full system depends on the performance of both components. The crosstalk benchmarks were lower when the thresholds for the respective primary muscle differed strongly from channel to channel. An example of such behaviour can be seen by comparing experiments "*A4_0519*" and "*A6_0512*". The thresholds in the first experiment were much further apart (TA on Ch1: 390 µA and G on Ch2: 650 µA) than in the latter (TA on Ch2: 758 µA and G on Ch4: 977 µA). This means that in the first example upon stimulating the gastrocnemius muscle on the second channel, just a small fraction of this current needs to stimulate on the first channel to activate the counteracting tibialis anterior muscle. As the thresholds were closer together in example "A6_0512", this fraction of current became larger and therefore the crosstalk benchmarks were more forgiving.

Model 2

Model 2 (table 15) assumed a linear interaction between the separate stimulation sites. These crosstalk benchmarks were considerably less forgiving than those obtained by model 1. This difference grows larger as the thresholds on the separate channels are further apart, because the currents on channels with lower thresholds are weighed more strongly in model 2. From this it can be derived, that the interaction between two stimulation sites becomes a bigger factor for the crosstalk current ratio in cases, where the thresholds vary greatly between channels. According to model 2, there is no lower crosstalk benchmark. This means, that an improved crosstalk coefficient will always bring about a higher selectivity of the full system. The large difference between the results from model 1 and model 2 show, that if further development of this system is pursued, the nature of the interaction between two stimulating sites should be thoroughly investigated. This could be done by performing experiments with a minimal version of the implant which only contains the nerve cuff electrode as well as some means to directly contact it. This implant would be much smaller and the rats would more likely survive for the intended duration of the experiment. In addition the measurement protocol could be shortened by skipping the stimulation with the long phase widths. Instead more measurements with short phase widths could be performed, thus providing more data points for smoother recruitment curves. The difference in the thresholds of fascicles of differing diameter and distance to electrode is larger for smaller pulse widths [18].

The effects of the crosstalk coefficient on the relationship between the selectivity of the full system and the crosstalk coefficient of the coupling array are summarized in Table 4. This data can provide valuable information for the further development of the system, as the crosstalk coefficients which can currently be supplied by the coupling array are larger than c_{high} and c_{M2}. This means that the limiting factor for the full system was the coupling array. The separate development of the coupling array could be partially performed in *ex vivo* experiments in a similar fashion to Kiele et al.[17], which are easier, cheaper and faster to carry out. Kiele et al. achieved a crosstalk coefficient of 86.5% (SD=1.3%)[17] for two channels with a similar coupling array under *ex vivo* conditions, which is similar to the coefficient of 97.4% (SD= 5.5%) that we achieved under *in vivo* conditions. However even the crosstalk coefficient under *ex vivo* conditions is still to large to be used in the full system selectively even if all issues arising through the implementation into a living system would have been solved. Due to the small sample size and the large spread of the results, it is difficult to predict the requirements for a future system. However, the lowest (i.e. strictest) crosstalk benchmark would

be 52% by model 1 and 23% by model 2. This corresponds to a current distribution of 66% / 34% (“primary channel” / “secondary channel”) for model 1 and 81% / 19% for model 2. Under these conditions all evaluated experiments which we performed would meet the requirement for selective stimulation. Model 1 predicts that at crosstalk coefficients below 37% the array design will no longer be the limiting factor. This corresponds to a current distribution of 72% / 27%.

11 Conclusion

A system for the selective stimulation of the gastrocnemius and the tibialis anterior muscle was examined *in vivo* in 10 female Sprague Dawley rats. It consisted of a pair of electrode arrays, one external and one implanted under the skin, as well as a multi channel cuff electrode, wrapped around the sciatic nerve and a headstage socket, mounted on the head, to connect the array and the cuff with the measurement equipment and to allow for separate analysis of the two components.

The required surgery and the experiments were very taxing on the animal subjects, and the average life expectancy was below the intended duration of the experiment. Therefore, the design of the implant should to be adjusted to be less invasive by reducing size and design.

The stimulation with the nerve cuff proved to be selective in 3 out of 7 animals. Out of this data the necessary quality of the input signal for the cuff electrode was determined, which would have to be supplied by the electrode array using two different models. The observed maximum values of crosstalk current leaking to the secondary channel were considerably higher than what could be offered by the array in its current design. We estimate that further development of the system needs to focus on reaching crosstalk currents at least below 52% and preferably below 37% before the other components become the limiting factors. Development of the electrode array could be performed in *ex vivo* experiments to facilitate the process and reduce costs in the number of test subjects, money and time.

Additionally the interaction of stimulation on multiple sites needs to be further investigated, as it can have a severe impact on the acceptable current ratio and could be used to produce better estimates of the allowed crosstalk current ratios. The development of the implant stability over time and the impact of healing around the implant needs to be further investigated as well.

The surface ground electrode proved to be an additional obstacle and additional experiments are necessary to investigate the issue. This requires for the animals to survive for the intended duration of the experiment, and therefore needs to be preceded by a redesign of the implant.

12 Outlook

For the further development of the system we suggest a process in several stages. Work on later stages should only be conducted after all milestones of the previous stage have been completed.

Stage 1

Coupling array: The coupling array should be developed under *ex vivo* conditions until at least the crosstalk benchmarks from Model 1 (crosstalk coefficient below 52%) are met.

General design: The implant needs to be redesigned, so that the expected lifetime of the test subjects is at least as long as the intended experiment duration. The size should be reduced to minimize the strain on the animal and the components. Elements permanently protruding the skin should be removed.

Stage 2

Coupling array: The coupling array should be tested under *in vivo* conditions and the crosstalk benchmark from Model 1 (crosstalk coefficient below 52%) should be aspired. Insulating the channels of the internal array should be considered as a means to achieve this goal.

Cuff electrode: The possibilities of steered currents similar to Tarler et al.[25] and Veraart et al.[26] should be explored and if possible implemented. Using the additional data the interaction during simultaneous stimulation at several sites should be analysed. This newly determined relationship could be used to replace the assumed linear relationship in Model 2 thus producing a more precise prediction of the necessary crosstalk coefficient. In addition the development of the selectivity over time should be investigated further.

Surface ground: The influence of the surface ground on the stimulation should be analysed, especially in regards to the possibility of using steering currents.

Stage 3

General design: Using the insights gained in the previous two stages the full system should be implanted and analysed under *in vivo* conditions similar to the experiments performed in this thesis. The performance of all components should be assessed separately as well as the performance of the system as a whole.

13 Bibliography

1. Arslan, O. *Neuroanatomical Basis of Clinical Neurology*. (Taylor & Francis Ltd, 2001).
2. Campbell, N. A. & Reece, J. B. *Biology*. (Pearson/Benjamin Cummings, 2005).
3. Nernst, W. Die elektromotorische Wirksamkeit der Jonen. in *Zeitschrift für Physikalische Chemie*, **4U.** (1889). doi:10.1515/zpch-1889-0412
4. Kandel, E. Principles of Neural Science. (McGraw-Hill-Companies, 2000)
5. Enderle, J. BIOELECTRIC PHENOMENA. in *Introduction to Biomedical Engineering* 627–691 (Elsevier, 2005). doi:10.1016/B978-0-12-238662-6.50013-6.
6. Pitta, M. D. Myelin and saltatory conduction. in *Dano Cerebral.* (JC Arango-Asprilla & L Olabarrieta-Landa eds., 2017).
7. Karpati, G., Hilton-Jones, D., Bushby, K. & Griggs, R. C. *Disorders of Voluntary Muscle*. (Cambridge University Press, 2009).
8. Beck, H., Anastasiadou, S. & Meyer zu Reckendorf, C. *Faszinierendes Gehirn*. (Springer Berlin Heidelberg, 2018). doi:10.1007/978-3-662-54756-4.
9. Bajd, T. & Munih, M. VI.2: Basic Functional Electrical Stimulation(FES) of Extremites – an Engineer's View. *Technol. Health Care Off. J. Eur. Soc. Eng. Med.* (2010) doi: 10.3233/THC-2010-0588.
10. Martin, R., Sadowsky, C., Obst, K., Meyer, B. & McDonald, J. Functional Electrical Stimulation in Spinal Cord Injury: From Theory to Practice. *Top. Spinal Cord Inj. Rehabil.* **18**, 28–33 (2012). doi:10.1310/sci1801-28
11. Rattay, F. *Electrical Nerve Stimulation*. (Springer Vienna, 1990). doi:10.1007/978-3-7091-3271-5.
12. Thakor, N. V., Wang, Q. & Greenwald, E. Bidirectional peripheral nerve interface and applications. in *2016 38th Annual International Conference of the IEEE Engineering in Medicine and Biology Society (EMBC)* 6327–6330 (IEEE, 2016). doi:10.1109/EMBC.2016.7592175.
13. Halaki, M. & Gi, K. Normalization of EMG Signals: To Normalize or Not to Normalize and What to Normalize to? in *Computational Intelligence in Electromyography Analysis - A Perspective on Current Applications and Future Challenges* (ed. Naik, G. R.) (InTech, 2012). doi:10.5772/49957.
14. Liu Shi Gan & Prochazka, A. Properties of the Stimulus Router System, a Novel Neural Prosthesis. *IEEE Trans. Biomed. Eng.* **57**, 450–459 (2010). doi: 10.1109/TBME.2009.2031427
15. Slaughter, M. S. & Myers, T. J. Transcutaneous Energy Transmission for Mechanical Circulatory Support Systems: History, Current Status, and Future Prospects. *J. Card. Surg.* **25**, 484–489 (2010). doi: 10.1111/j.1540-8191.2010.01074.x
16. Erfani, R., Marefat, F., Sodagar, A. M. & Mohseni, P. Transcutaneous capacitive wireless power transfer (C-WPT) for biomedical implants. in *2017 IEEE International Symposium on Circuits and Systems (ISCAS)* 1–4 (IEEE, 2017). doi:10.1109/ISCAS.2017.8050940.
17. Kiele, P. *et al.* Neural Implants Without Electronics: A Proof-of-Concept Study on a Human Skin Model. *IEEE Open J. Eng. Med. Biol.* **1**, 91–97 (2020). doi:10.1109/OJEMB.2020.2981254

18. Grill, W. M., Norman, S. E. & Bellamkonda, R. V. Implanted Neural Interfaces: Biochallenges and Engineered Solutions. *Annu. Rev. Biomed. Eng.* **11**, 1–24 (2009). doi:10.1146/annurev-bioeng-061008-124927

19. Tanabe, Y. *et al.* High-performance wireless powering for peripheral nerve neuromodulation systems. *PLOS ONE* **12**, (2017). doi:10.1371/journal.pone.0186698

20. Guillen, J. FELASA guidelines and recommendations. *J. Am. Assoc. Lab. Anim. Sci.* **51**, (2012).

21. Polasek, K. H., Hoyen, H. A., Keith, M. W. & Tyler, D. J. Human Nerve Stimulation Thresholds and Selectivity Using a Multi-contact Nerve Cuff Electrode. *IEEE Trans. Neural Syst. Rehabil. Eng.* **15**, 76–82 (2007). doi:10.1109/TNSRE.2007.891383

22. Peckham, P. H., Poon, C. W., Ko, W. H., Marsolais, E. B. & Rosen, J. J. Multichannel Implantable Stimulator for Control of Paralyzed Muscle. *IEEE Trans. Biomed. Eng.* **BME-28**, 530–536 (1981). doi:10.1109/TBME.1981.324740

23. Krenn, M., Hofstoetter, U. S., Danner, S. M., Minassian, K. & Mayr, W. Multi-Electrode Array for Transcutaneous Lumbar Posterior Root Stimulation: Multi-Electrode Array. *Artif. Organs* **39**, 834–840 (2015). doi:10.1111/aor.12616

24. The Ohio State University. Vet-Guideline 19-013, Rodent Survival Surgery Guidelines. (2019)

25. Tarler, M. D. & Mortimer, J. T. Selective and independent activation of four motor fascicles using a four contact nerve-cuff electrode. *IEEE Trans. Neural Syst. Rehabil. Eng.* **12**, 251–257 (2004). doi:10.1109/TNSRE.2004.828415

26. Veraart, C., Grill, W. M. & Mortimer, J. T. Selective control of muscle activation with a multipolar nerve cuff electrode. *IEEE Trans. Biomed. Eng.* **40**, 640–653 (1993).

14 Appendix

14.1 Timeline and experiment overview

The following timetable gives an overview on the performed measurements.

Timeline of the measurements

Experiment	Surgery	Measurement	Days
A4_0415	15.04.21	15.04.21	0
A4_0428	15.04.21	28.04.21	13
A4_0519	15.04.21	16.05.21	31
A4_0527	15.04.21	27.05.21	42
A4_0610	15.04.21	10.06.21	56
A4_0705	15.04.21	05.07.21	81
A3_0428	15.04.21	28.04.21	13
A5_0429	29.04.21	29.04.21	0
A5_0512	29.04.21	12.05.21	13
A5_0527	29.04.21	27.05.21	28
A6_0429	29.04.21	29.04.21	0
A6_0512	29.04.21	12.05.21	13
A6_0519	29.04.21	19.05.21	20
A7_0505	05.05.21	05.05.21	0
A7_0519	05.05.21	19.05.21	14
A7_0602	05.05.21	02.06.21	28
A7_0610	05.05.21	10.06.21	36
A8_0505	05.05.21	05.05.21	0
A9_0520	20.05.21	20.05.21	0
A9_0602	20.05.21	02.06.21	13
A10_0520	20.05.21	20.05.21	0

Table I: Overview of the timeline of the performed experiments. Days refers to the number of days after surgery

14.2 Results for all CorTec experiments

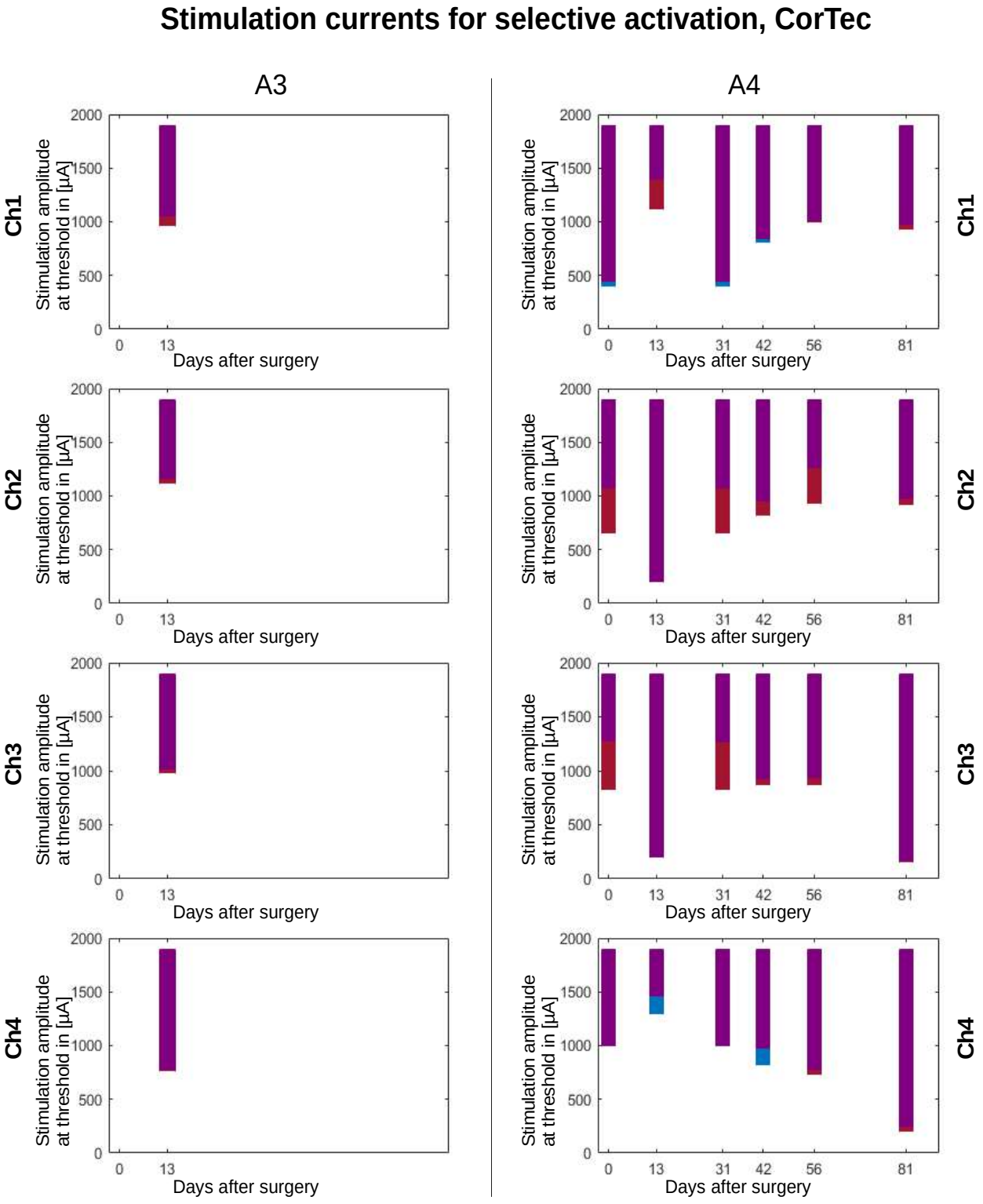

Figure I: Development of activation currents for selective stimulation over time after surgery. Red areas show currents which stimulate only the gastrocnemius muscle while blue areas show currents which only stimulate the tibialis anterior muscle. Purple areas activate both muscles. CorTec setup

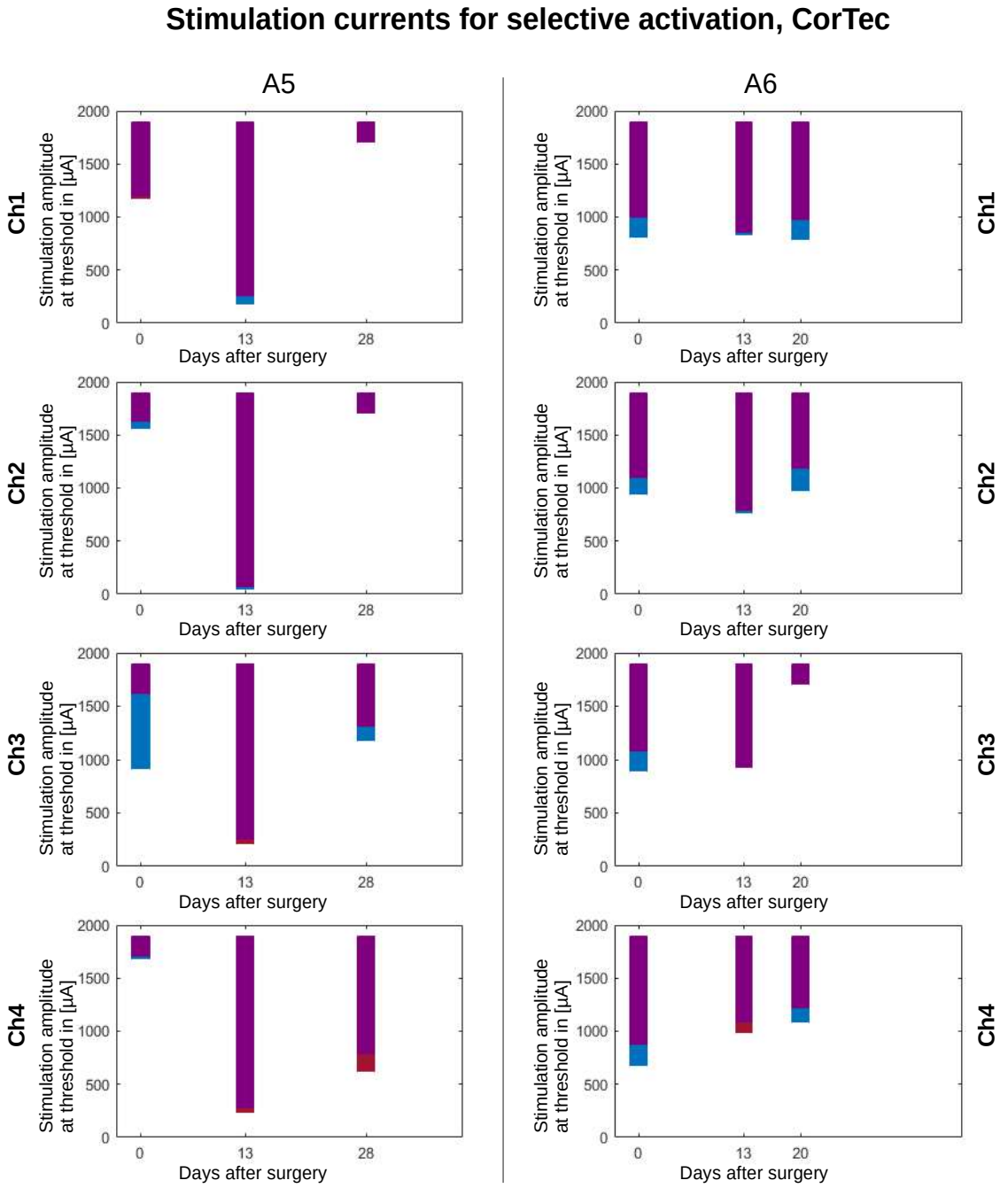

Figure II: Development of activation currents for selective stimulation over time after surgery. Red areas show currents which stimulate only the gastrocnemius muscle while blue areas show currents which only stimulate the tibialis anterior muscle. Purple areas activate both muscles. CorTec setup

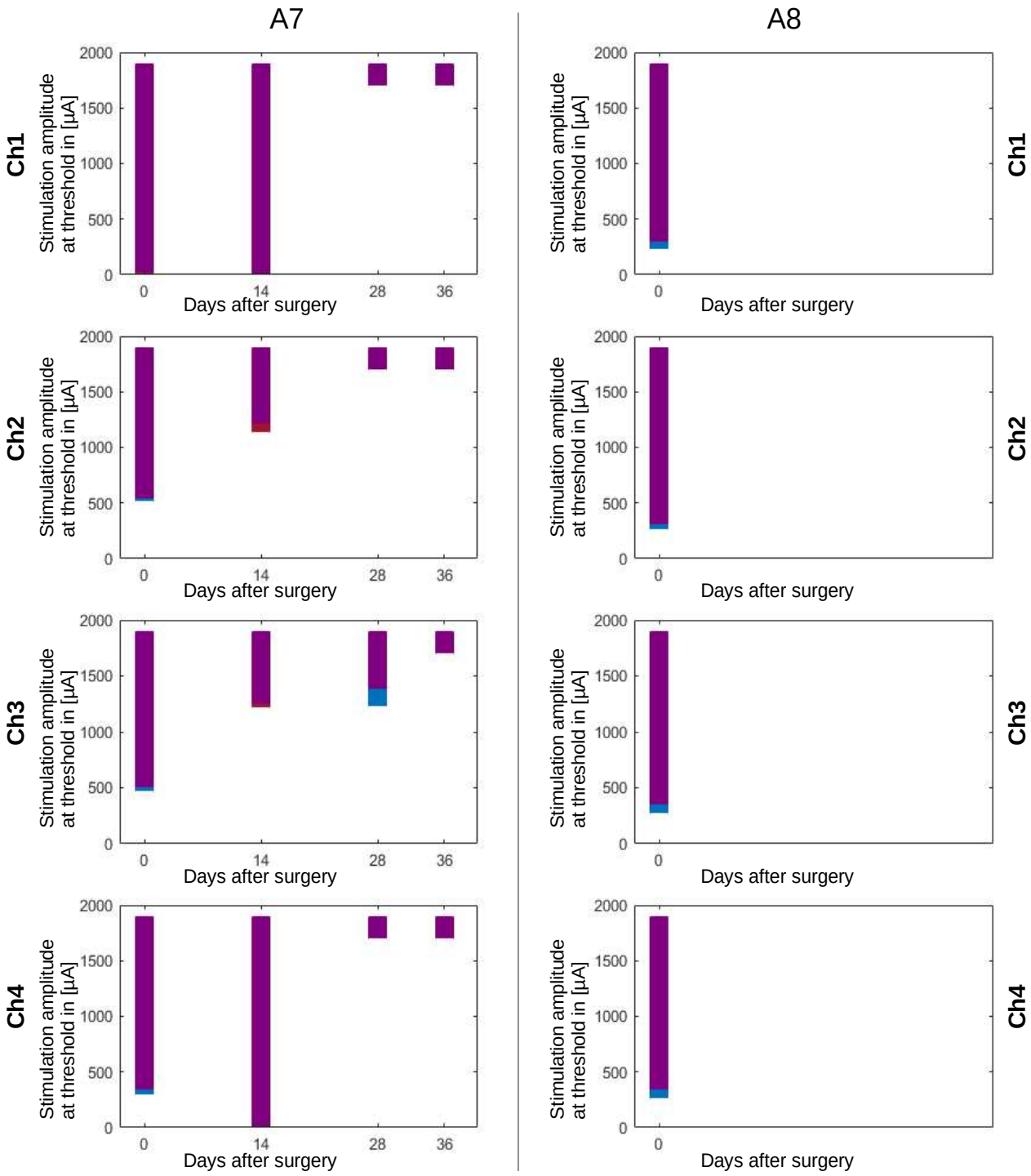

Figure III: Development of activation currents for selective stimulation over time after surgery. Red areas show currents which stimulate only the gastrocnemius muscle while blue areas show currents which only stimulate the tibialis anterior muscle. Purple areas activate both muscles. CorTec setup

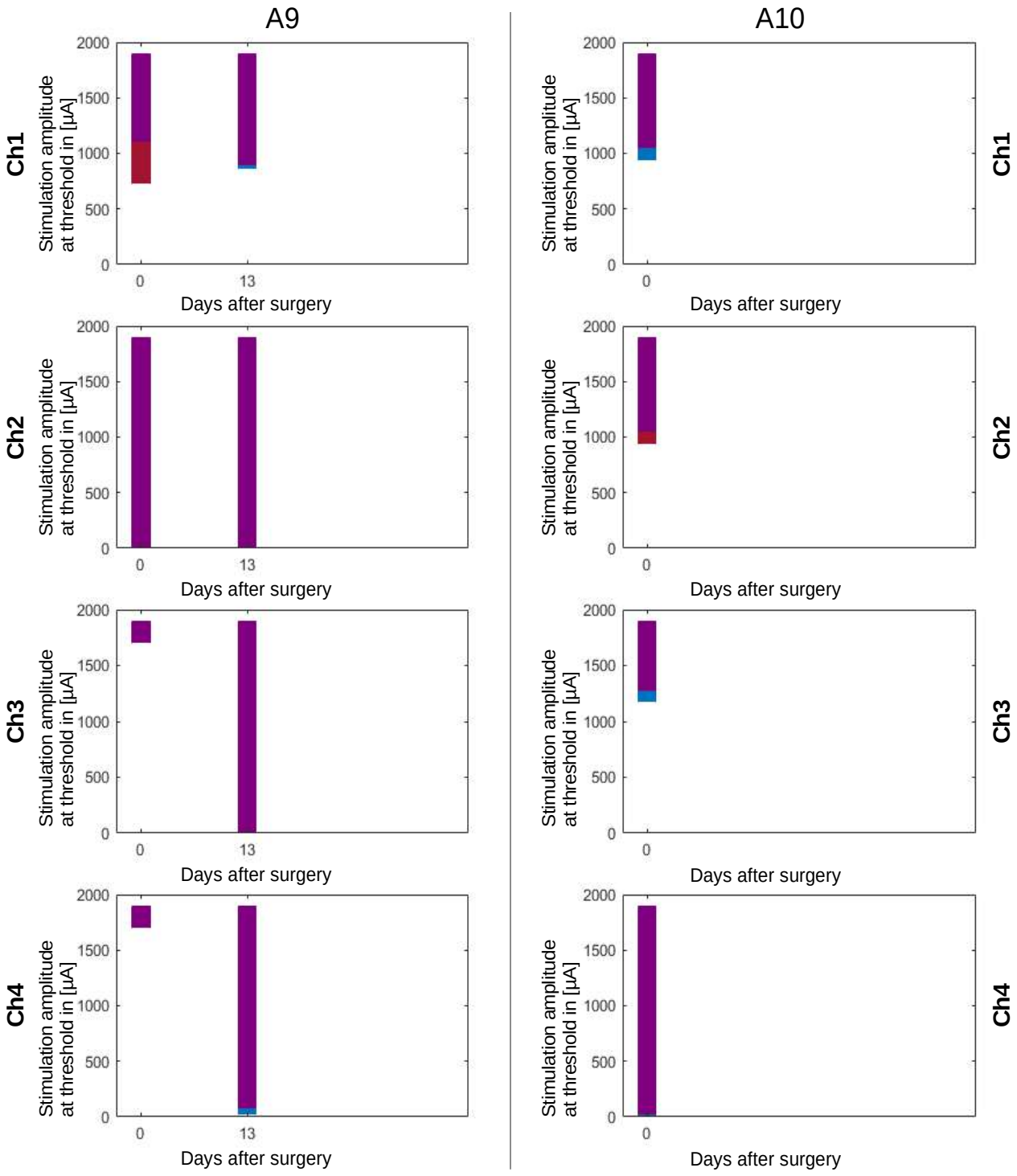

Figure IV: Development of activation currents for selective stimulation over time after surgery. Red areas show currents which stimulate only the gastrocnemius muscle while blue areas show currents which only stimulate the tibialis anterior muscle. Purple areas activate both muscles. CorTec setup

14.3 Results for Isis experiments

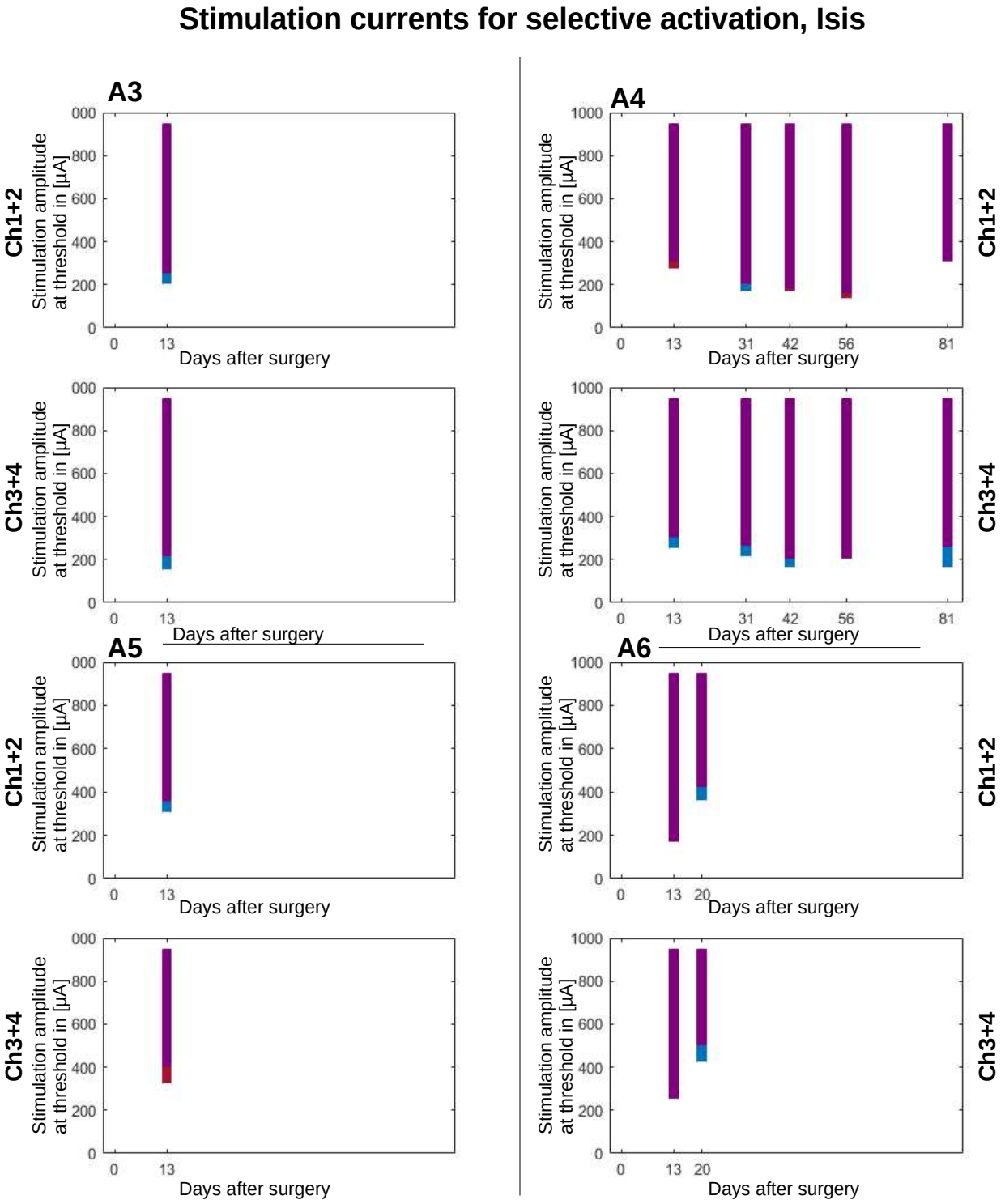

Figure V: Development of activation currents for selective stimulation over time after surgery. Red areas show currents which stimulate only the gastrocnemius muscle while blue areas show currents which only stimulate the tibialis anterior muscle. Purple areas activate both muscles. Isis setup

Stimulation currents for selective activation, Isis

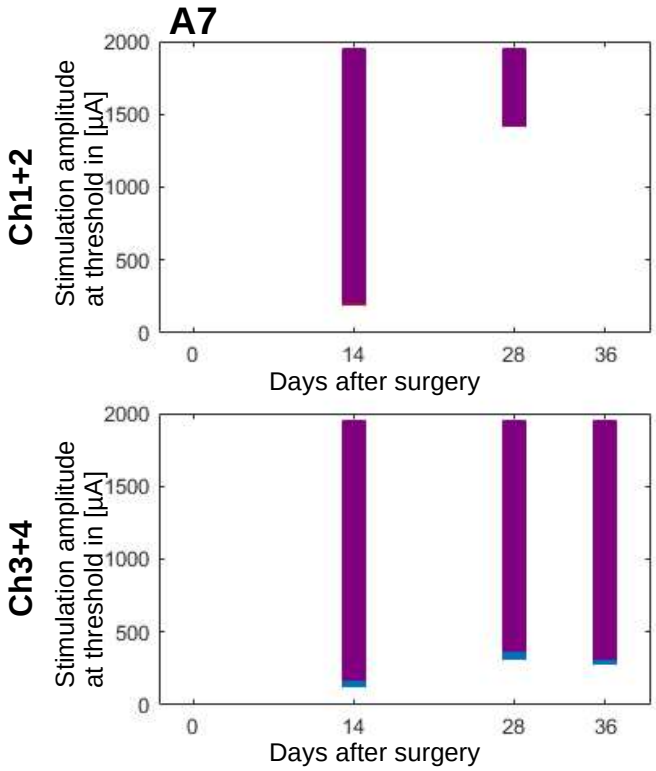

Figure VI: Development of activation currents for selective stimulation over time after surgery. Red areas show currents which stimulate only the gastrocnemius muscle while blue areas show currents which only stimulate the tibialis anterior muscle. Purple areas activate both muscles. Isis setup

14.4 Results for Isis experiments + surface ground

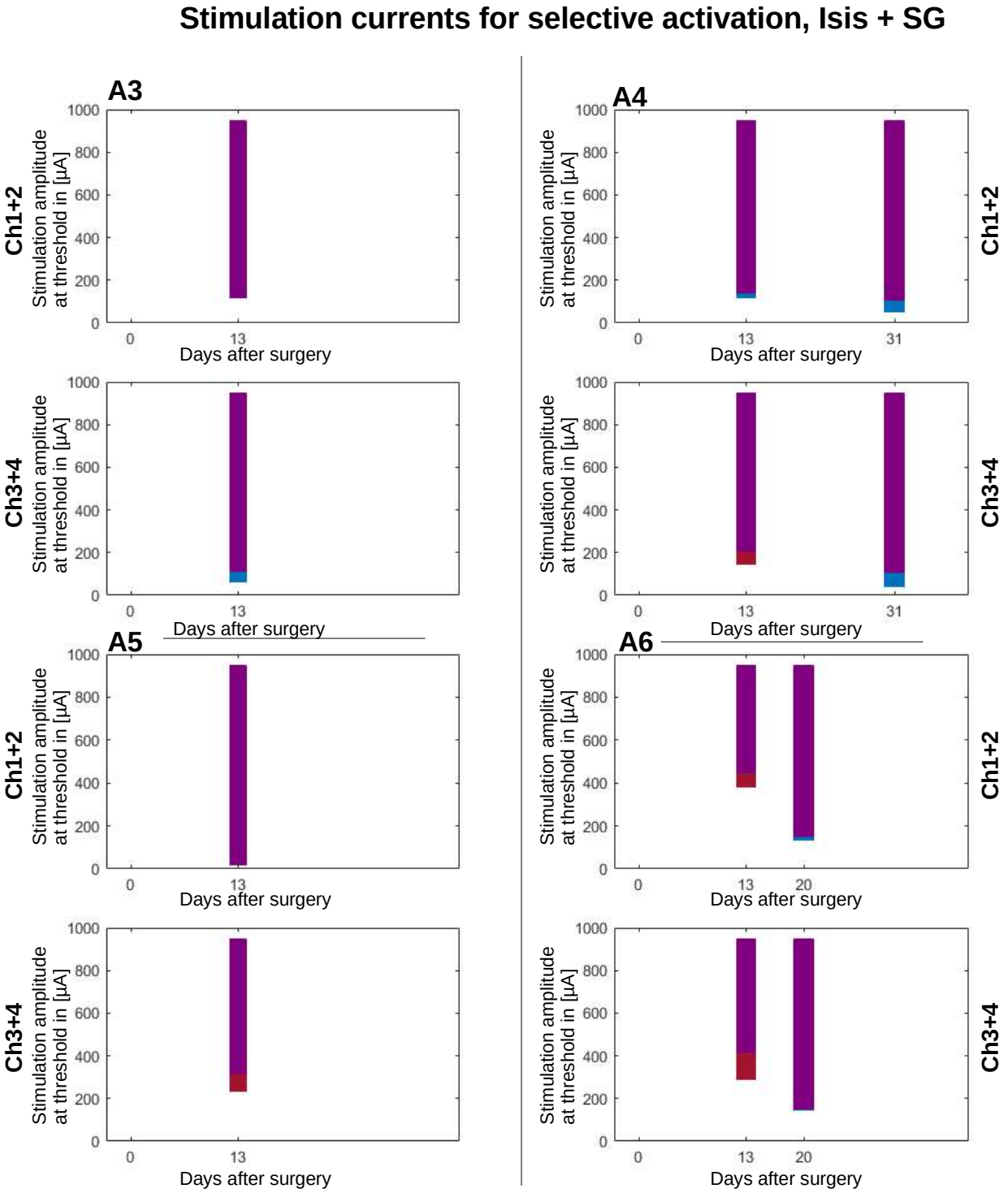

Figure VII: Development of activation currents for selective stimulation over time after surgery. Red areas show currents which stimulate only the gastrocnemius muscle while blue areas show currents which only stimulate the tibialis anterior muscle. Purple areas activate both muscles. The first two and the last two channels of the cuff are connected. Isis setup with surface ground electrode

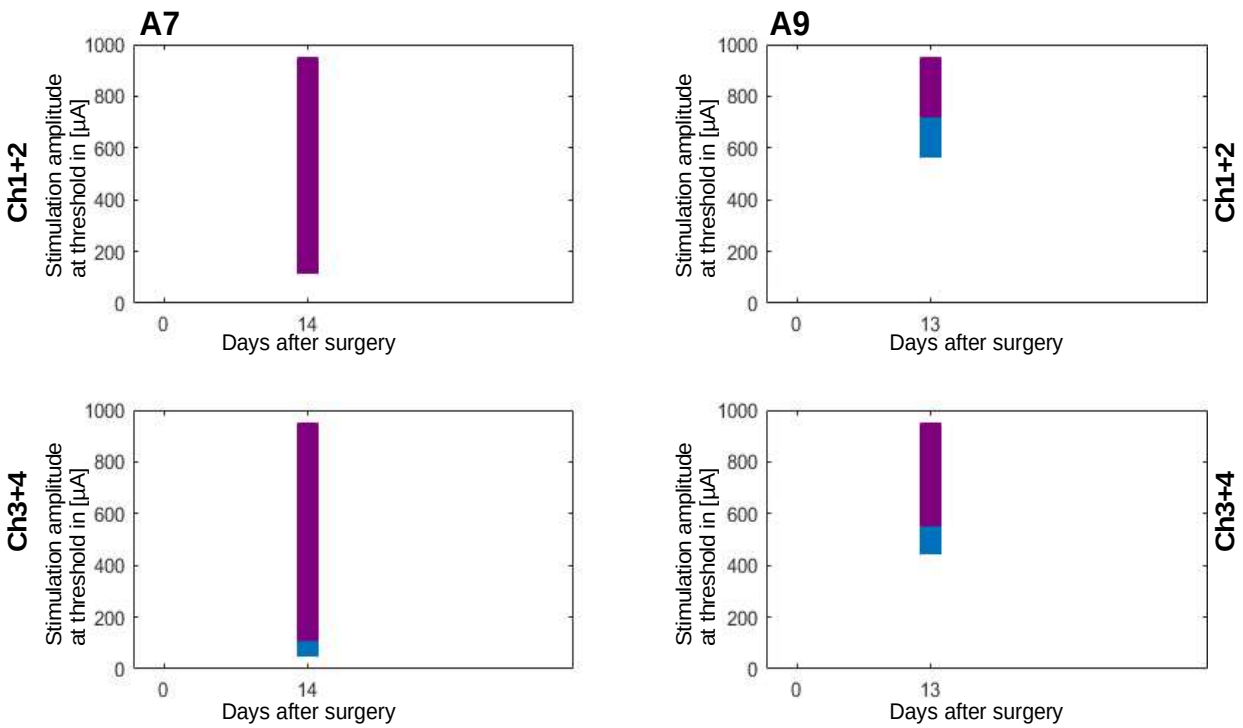

Figure VIII: Development of activation currents for selective stimulation over time after surgery. Red areas show currents which stimulate only the gastrocnemius muscle while blue areas show currents which only stimulate the tibialis anterior muscle. Purple areas activate both muscles. The first two and the last two channels of the cuff are connected. Isis setup with surface ground electrode

14.5 Matlab script, Model 2

(Matlab version R2020b)

```
clear all
%declare thresholds in µA
tg1= 859;
tg2= 962;
ta1= 914;
ta2= 817;
crosstalk= linspace(100,1,100);
crosstalk= crosstalk/100;
currents= linspace(1,2000,200);
for i= 1:length(crosstalk)
    c= crosstalk(i);
    %Channel 1 check
    i1= currents;
    i2= c* currents;
    activationG1= i1/tg1 + i2/tg2;
    activationA1= i1/ta1 + i2/ta2;
    a= find(activationG1>1,1);
    b= find(activationA1>1,1);
    thrG1(i)= currents(a);
    thrA1(i)= currents(b);
    clear a b
    %Channel 2 check
    i1= c * currents;
    i2= currents;
    activationG2= i1/tg1 + i2/tg2;
    activationA2= i1/ta1 + i2/ta2;
    a= find(activationG2>1,1);
    b= find(activationA2>1,1);
    thrG2(i)= currents(a);
    thrA2(i)= currents(b);
    clear a b
end
checker1=thrG1-thrA1;
checker2=thrG2- thrA2;
checksum= checker1 .*checker2;
m= find (checksum<0, 1);
limit= crosstalk(m)
```